NAWCWD TP 8839

Geomorphic Map of the China Lake Basin Below 700 m in Support of Cultural Resource Management at Naval Air Weapons Station China Lake

Prepared by
Thomas Bullard, Steven Bacon, Kenneth Adams, and David Decker
Naval Earth Sciences and Engineering Program
Desert Research Institute, Nevada System of Higher Education
Division of Hydrological Science
Reno, Nevada

MAY 2019

NAVAL AIR WARFARE CENTER WEAPONS DIVISION
CHINA LAKE, CA 93555-6100

Naval Air Warfare Center Weapons Division

FOREWORD

This report documents the development of a geomorphic map of sufficient detail to be used in the accurate association of archaeological sites and site types with specific landforms leading toward a geomorphic-based archaeological favorability model (AFM) within the China Lake Ranges. The primary requirement for developing a geomorphic-based tool is a detailed geomorphic map that depicts the distribution of different age landscape components, which until now has not been available at the Naval Air Weapons Station (NAWS) China Lake. A geomorphic-based AFM has the potential to provide cultural resource managers and installation managers with a method to enhance strategies and decision-making with regard to assessing resource allocation for cultural resource management. The map product of this report, covering the portion of the China Lake basin below the 700 m (2,297 ft) mean sea level elevation contour provides the foundational framework for assessing associations among mappable landscape components (e.g., alluvial fans, shoreline features) and prehistoric cultural resources at NAWS China Lake.

The work upon which this report is based has been conducted as part of the Naval Air Warfare Center Weapons Division (NAWCWD) Range Sustainment Office's continuing efforts to define and mitigate potential mission encroachments. The work outlined in the report is intended to both help mitigate future impacts to the NAWCWD China Lake Research, Development, Test, and Evaluation (RDT&E) mission, and to also provide a tool to enable informed decisions relative to planning and conduct of range operations.

This report has been reviewed by M. L. Boggs.

Approved by
T. DOWD, *Director*
NAVAIR Ranges
08 May 2019

Under authority of
W. S. DILLON
RDML, U.S. Navy
Commander

Released for publication by
J. L. JOHNSON
Director for Research and Engineering

NAWCWD Technical Publication 8839

Published by.....Technical Communication Office
Collation.....Cover, 39 leaves
First printing.....4 paper, 6 electronic media

REPORT DOCUMENTATION PAGE

Form Approved
OMB No. 0704-0188

1. REPORT DATE *(DD-MM-YYYY)*	2. REPORT TYPE	3. DATES COVERED (From - To)
08-05-2019	Final evaluation report	1 October 2012 – 30 September 2015

4. TITLE AND SUBTITLE

Geomorphic Map of the China Lake Basin Below 700 m in Support of Cultural Resource Management at Naval Air Weapons Station China Lake (U)

5a. CONTRACT NUMBER
N/A

5b. GRANT NUMBER
N/A

5c. PROGRAM ELEMENT NUMBER
N/A

6. AUTHOR(S)

Thomas F. Bullard, Steven N. Bacon, Kenneth D. Adams and David L. Decker

5d. PROJECT NUMBER
N/A

5e. TASK NUMBER
N/A

5f. WORK UNIT NUMBER
N/A

7. PERFORMING ORGANIZATION NAME(S) AND ADDRESS(ES)

Desert Research Institute
Nevada System of Higher Education
2215 Raggio Parkway
Reno, NV 89512

8. PERFORMING ORGANIZATION REPORT NUMBER
50011

9. SPONSORING/MONITORING AGENCY NAME(S) AND ADDRESS(ES)

Naval Air Warfare Center Weapons Division
NAVAIR Ranges (Code 52000MD)
130 Easy Rd Stop 3002
China Lake, CA 93555-6109

10. SPONSOR/MONITOR'S ACRONYM(S)
NAWCWD

11. SPONSOR/MONITOR'S REPORT NUMBER(S)
NAWCWD TP 8839

12. DISTRIBUTION/AVAILABILITY STATEMENT

DISTRIBUTION STATEMENT A. Approved for public release; distribution is unlimited.

13. SUPPLEMENTARY NOTES

14. ABSTRACT

(U) Geomorphic mapping of China Lake basin provides the most detailed geomorphic map available for the China Lake basin. The geomorphic map represents a major step forward in laying the foundation for assessing associations among mappable landscape components (e.g., alluvial fans, shoreline features) and prehistoric cultural resources at Naval Air Weapons Station (NAWS) China Lake. The primary objective of the Phase II project was to generate a highly detailed geomorphic map for the area below the 700 m contour elevation at China Lake. About 59 percent of the area consists of landforms younger than early Holocene, of which ~11 percent range in age from 8,200 to 4,200 calendar years before present (cal yr B.P.). The remaining 48 percent range in age from 4200 to 2014 A.D. and consist of hillslope, alluvial, eolian, fluvial, and playa feature types. The other 41 percent of the area consist of landforms that have an age of 15,000 – 13,700 cal yr B.P., which consist of intermediate-age alluvial fans, lacustrine, and deltaic feature types.

15. SUBJECT TERMS

China Lake Basin, Cultural Resource Management, Geomorphic Map, NAWS China Lake

16. SECURITY CLASSIFICATION OF:			17. LIMITATION OF ABSTRACT	18. NUMBER OF PAGES	19a. NAME OF RESPONSIBLE PERSON
a. REPORT	b. ABSTRACT	c. THIS PAGE			M. L. Boggs
UNCLASSIFIED	UNCLASSIFIED	UNCLASSIFIED	SAR	76	19b. TELEPHONE NUMBER *(include area code)* (760) 939-4404

CONTENTS

Figures:

Tables:

ACKNOWLEDGEMENTS

This work was conducted in collaboration with Matt Boggs, China Lake Ranges Chief Engineer, Naval Air Warfare Center Weapons Division. We gratefully acknowledge the following: Dr. Amanda Keen-Zebert, Director of the Desert Research Institute (DRI) E. L. Cord Luminescence Laboratory for optically stimulated luminescence (OSL) age determinations; Charles Morton, DRI for assistance with principal component analysis of spectral imagery; and Heather Green, DRI for assistance with ArcGIS geodatabase management of the geomorphic map.

LIST OF ACRONYMS

AFM	Archaeological Favorability Model
ALFZ	Airport Lake fault zone
CRM	Cultural Resources Management
DoD	Department of Defense
DRILL	Desert Research Institute E. L. Cord Luminescence Laboratory
IRSL	Infrared Stimulated Luminescence
LLFZ	Little Lake fault zone
NAWS	Naval Air Weapons Station
SERDP	Strategic Environmental Research and Development Program

This page intentionally left blank.

EXECUTIVE SUMMARY

The primary goal of the Phase II geomorphic mapping project was to generate a geomorphic map of sufficient detail to be used in the accurate association of archaeological sites and site types with specific landforms leading toward a geomorphic-based archaeological favorability model (AFM). An AFM will enable rapid and effective assessment of areas not yet evaluated for cultural resources, thereby reducing the frequency of use of "boots-on-ground" field survey methods, which in turn reduces the impact to fiscal resources and range operations.

The geomorphic map also will be an important resource that can be used for a number of different purposes in addition to its cultural resource application. These uses may include, but not limited to, the assessment of natural hazards in China Lake basin such as flooding hazard, dust emission hazard, and hazards or threats associated with eolian sand transport, as well as assessing geomorphic influences on the distribution of floral and faunal populations and geomorphic processes that have bearing on the siting of critical facilities. The geomorphic map also forms an important framework and basis for assessing potential landscape changes that may be associated with changing climate.

The Phase II geomorphic map product represents the integration of Phase I and Phase II mapping efforts. The mapping of China Lake basin was divided into two phases to accommodate funding availability. The completed map, although preliminary pending on the ground field checking of key locations, provides the most detailed geomorphic map available for the China Lake basin. The geomorphic map represents a major step forward in laying the foundation for assessing associations among mappable landscape components (e.g., alluvial fans, shoreline features) and prehistoric cultural resources at Naval Air Weapons Station (NAWS) China Lake. The primary objective of the Phase II project was to generate a highly detailed geomorphic map for the area below the 700 m contour elevation at China Lake.

This report presents Phase II results of geomorphic mapping below the 700 m elevation contour in the China Lake basin in Indian Wells Valley. Phase II mapping was performed by a combination of manually digitizing geomorphic contacts onto high-resolution georeferenced aerial imagery in an ArcGIS database at a variable scale ranging from 1:2000 and 1:8000; Principal Component Analysis (PCA) contours were utilized for high-albedo areas having high contrast-reflectance. PCA had limited effectiveness in areas having low-contrast surface reflectance and was not used for piedmont mapping.

The Phase II map area has many of the same low-gradient, basin floor geomorphic features found below 665 m and previously mapped during Phase I; however, because of the relative higher topographic relief within the Phase II map area, a more diverse range of surface ages and feature types were identified than previously. Some of the older landform features identified around 700 m are the product of both internal and external paleohydrologic events (i.e., lake-level fluctuations and large floods) that have influenced the landscape history of China Lake basin. As a result, key areas above the 700 m contour were investigated to provide a larger areal and interbasin context of the geomorphology identified in China Lake basin (see Appendix B). The geomorphic map of China Lake basin below 700 m contour is presented on Plate 1 and is available as an ArcGIS geodatabase. Prominent erosional shoreline features are recorded in the landscape as bedrock

platforms and truncated alluvial fans at elevations of 700, 690, 683, and 670 m. Playas, recessional beach plains and lake plains, fluvial complexes and alluvial fans are recognized in much of the basin despite the ubiquitous cover of eolian sand.

Nine primary landform feature types were identified in the map area (390 km^2) including: hillslope, alluvial fan, deltaic, eolian, fluvial, lacustrine, playa, bedrock, and anthropogenic. These primary feature types were further separated into forty-eight distinct geomorphic units with a corresponding surface age when applicable (Table 2). The three most prevalent landform feature types in the map area are alluvial fan (37%), eolian (14%), and fluvial (13%) with the remaining feature types comprising of playa (12%), deltaic (9%), lacustrine (11%), and bedrock (1.3%), plus anthropogenic (0.6%) and hillslope (0.3%).

About 59 percent of the area consists of landforms younger than early Holocene, of which ~11 percent range in age from 8,200 to 4,200 cal yr B.P. The remaining 48 percent range in age from 4,200 to 2014 A.D. and consist of hillslope, alluvial, eolian, fluvial, and playa feature types. The other 41 percent of the area consist of landforms that have an age of 15,000 – 13,700 yr cal B.P., which consist of intermediate-age alluvial fans, lacustrine, and deltaic feature types. The results of previously pending luminescence analysis in March 2015 have been included in an addendum to the report dated October 2018.

With the mapping accomplished, the longer-term goal will be to analyze documented associations between the types and ages of desert landforms and the occurrence of prehistoric archaeology leading to development of a geomorphic-based tool to assess archaeological favorability within the landscape.

(**NOTE**: The contents of this document are reproduced in facsimile.)

1.0 PROJECT GOALS AND OBJECTIVES

The primary objective of this phase of the project was to generate a geomorphic map of sufficient detail to be used in the accurate association of archaeological sites and site types with specific landforms leading toward a geomorphic-based archaeological favorability model (AFM). An AFM will enable rapid and effective assessment of areas not yet evaluated for cultural resources, thereby reducing the frequency of use of 'boots-on-ground' field survey methods, which in turn reduces the impact to fiscal resources and range operations. Because an AFM is designed to be approachable by a broad set of skillsets and knowledge, the application of an AFM will lead to improved communications and buy-in amongst stakeholders. To achieve the objective of an AFM, the longer-term goals that must be realized are to analyze documented associations between the types and ages of desert landforms and the occurrence of cultural resources and then develop a geomorphic-based tool to be used to support cultural resource management at Naval Air Weapons Station (NAWS) China Lake. The primary requirement for developing a geomorphic-based tool is a detailed geomorphic map that depicts the distribution of different age landscape components, which until now has not been available at NAWS China Lake.

The relation between landscape age and archaeological sites is well established, although the application of the practice is not widespread in the arid southwestern U.S. but is gaining acceptance (*e.g.*, Waters, 1992; Ruiz, 2002; McDonald and Bullard, 2003; McDonald *et al.*, 2004; Bullard, 2010; Bullard and Bacon, 2010; Bullard *et al.*, 2010; Bullard *et al.*, 2015). A geomorphic-based AFM has the potential to provide cultural resource managers and installation managers with a method to enhance strategies and decision-making with regard to assessing resource allocation for cultural resource management. For example, where and how to best spend fiscal and labor resources, such as the location and intensity of archaeological surveys and mitigation activities, with the ultimate goal being to identify areas and the likelihood of finding prehistoric cultural materials in those areas at NAWS China Lake.

Production of the detailed geomorphic map was accomplished in two phases to accommodate funding availability. Phase I mapping of 110 km^2 was completed in FY 2012 for that portion of the China Lake basin below the 665 m elevation contour (Adams *et al.*, 2012a). The Phase II map (Plate 1) and map unit descriptions (Appendix A), completed in FY 2015, include the area (280 km^2) at China Lake below the 700 m elevation contour. The integrated Phase I and Phase II map product provides the foundational framework for assessing associations among mappable landscape components (*e.g.*, alluvial fans, shoreline features) and prehistoric cultural resources at NAWS China Lake. The map presented in this report should be considered preliminary pending on the ground field checking and verification of key geomorphic features.

2.0 INTRODUCTION

Effective stewardship, management of cultural and biological resources, and sustainable operational usage of range lands is critical to the mission of the U.S. military. Continued use of range lands requires compliance with state and federal regulations. Federal law requires inventorying historic properties before land can be used (Section 106 of the National Historic Preservation Act of 1966 [Public Law 89-665]). Traditional archaeological inventory methods (*i.e.*, pedestrian survey) are time- and labor-intensive, leading to a backlog of access-restricted areas in need of archaeological survey. One solution to this problem is to increase inventory efficiency by focusing survey efforts on those areas having high potential of containing cultural resources, and reducing the amount of time that is spent surveying areas with low potential. This could be achieved by implementing an AFM model consisting of a database or model that relates cultural resource parameters with quickly observed or surveyed land characteristics—typically environmental and/or geomorphological—to enable the site potential of locales to be assessed and ranked based on their environmental characteristics or geomorphic setting. Characterizing archaeological potential requires incorporation of key geomorphic variables to determine how the evolution of the land surface has contributed to the location and preservation (*i.e.*, site stability) of cultural features. Moreover, incorporation of the desert geomorphic environment into cultural resource surveys can also provide information in support of sampling strategies for determining the presence of buried cultural materials.

The topic of cultural resources management (CRM) on military installations has been the subject of several Department of Defense (DoD) workshops focusing on aspects identified in a workshop sponsored by DoD Strategic Environmental Research and Development Program (SERDP) and the Legacy Resource Management Program (Briuer *et al.*, 2000). During the past several decades, the science of geomorphology and soils has advanced to the point of demonstrating unique and predictable relationships between temporally and spatially variable landscape components and soils, hydrology, vegetation, geology, and prehistoric cultural resources (Bullard *et al.*, 2009, 2010). Recent research on military lands in arid regions has added to our knowledge of soil-geomorphic processes, landscape evolution, and linkage to distribution and preservation of cultural resources. Although several workshops addressed focus areas such as the "Find-It", "Conserve/Preserve It", Manage-It", and "Apply-It" (Briuer *et al.*, 2000), and predictive modeling workshops of Altschul *et al.* (2004), Limp (2006) and Lione (2007), a full integration of geology and geomorphology into cultural resource management models to support the military mission has not been undertaken (Bullard et al, 2009). This project at NAWS China Lake is an opportunity to demonstrate and apply geoarchaeological techniques to enhance cultural resource management on the range.

3.0 PREVIOUS WORK AT NAWS CHINA LAKE

Most archaeological and paleontological studies conducted on the history of China Lake basin have focused on the effect of paleoenvironmental change on Native American populations (Davis, 1978; Meyer *et al.*, 2011). Emma Lou Davis and numerous colleagues performed extensive archaeological and paleontological surveys, excavations, floral and faunal analysis, and radiocarbon dating in the late 1960s and early 1970s (Davis, 1975, 1978). These workers also focused on paleo-environmental changes at China Lake in order to provide context for the archaeological sites and floral and faunal remains (Davis, 1975).

Radiocarbon dating (typical applicable range >300 years and <55,000 years) is an isotopic method for dating organic matter that contains carbon isotopes acquired through natural growth processes and/or geochemical cycling (e.g., charcoal, wood, bone, macrofossil plant material, peat, pedogenic carbonate, shells, tufa) (see Trumbore, 2000, for a discussion of radiocarbon dating). The method is based on the radioactive decay of ^{14}C (half-life 5,730 years) ^{14}N. Two methods are employed, one that involves measuring the activity of ^{14}C of a sample by radioactive decay counting and the other by measuring individual ions of ^{14}C using accelerator mass spectrometry. Conventional radiocarbon ages are, by convention, reported as radiocarbon years before present (^{14}C yr B.P.) relative to 1950. Limitations of the method include variations of ^{14}C in atmospheric CO_2 in the past and require calibration to existing tree ring records to determine the calendar year associated with the radiocarbon age (Trumbore, 2000). Calibrated radiocarbon ages are reported as calendar years before present (cal yr B.P.). By convention, both radiocarbon and calibrated ages are initially presented together; subsequent reference to radiocarbon age is presented as the calendar year and considered to be the age of the material dated.

Because most of the Davis (1978) radiocarbon dates were generated on carbonate nodules, bulk soil samples, and tufa carbonate, subsequent paleo-environmental reconstructions were hampered by apparent chronologic inversions resulting from radiocarbon dates in conflict with the stratigraphy. This is primarily because tufa, carbonate nodules, and soil carbon have been demonstrated to be unsuitable for numerical dating by the radiocarbon method because these datable materials are susceptible to contamination with older or younger carbon (*e.g.*, Bischoff *et al.*, 1993; Trumbore, 2000).

Early in the stages of archaeological, paleontological, and environmental studies in the China-Searles lake basin, Davis (1975) and others (*e.g.*, Smith, 1968) had recognized the importance of shoreline features as chronological markers in the landscape. Davis (1978) dated shoreline features and late Pleistocene lake highstands from two radiocarbon samples on tufa. One sample collected at an elevation of about 681 m returned ages of 12,970 $\pm$ 150 ^{14}C yr B.P. (radiocarbon years before present) (~15,540 cal yr B.P.) and 11,870 $\pm$ 120 ^{14}C yr B.P. (~13,730 cal yr B.P.). More recent dating of a tufa sample collected at the late Pleistocene highstand (~690 m) returned an age of 12,400 $\pm$ 100 ^{14}C yr B.P. (~14,450 cal yr B.P.) (Lin *et al.*, 1998), which is similar in age to the dates Davis (1978) obtained for the shoreline feature at 681 m. The implication of dating tufa, even though the open geochemical system of tufas can be problematic, independent dating of

China Lake tufa samples returned similar dates. Until additional numerical age dating is performed, we tentatively accept these dates to be estimates of the age for the two high shorelines at China Lake.

Giambastiani and Bullard (2010) excavated three trenches along the northeast edge of China Lake playa at elevations around 668 m. Two localized sandy deposits in the form of beach ridges were exposed in one of the trenches and were sampled for luminescence dating. Depending on how the luminescence dates are interpreted, however, the stratigraphically lower beach deposit dated from either 8,000 or 11,000 years ago and the apparently younger beach deposit dates from either 15,900 or 11,000 years ago. Although these estimates overlap, the results at this time are considered ambiguous because of the possibility of an age inversion.

Meyer *et al.* (2011) present a synthesis of the history of China Lake based on extensive field investigations, radiocarbon dating, and reviews of previous work as part of the Department of Defense Legacy Management Program. Their field work involved a combination of outcrop studies along the paleo-Owens River channel upstream from China Lake and in the relatively small tributaries flowing into Indian Wells Valley from the adjacent Sierra Nevada, including coring efforts adjacent to China Lake, as well as investigating shorelines in Salt Wells Valley and revisiting stratigraphy in Poison Canyon. Meyer *et al.* (2011) also reviewed previous studies in the region (including many difficult-to-obtain technical reports) and compiled an extensive list of radiocarbon ages from published and unpublished studies from the region. Although Meyer *et al.* (2011) contains many site-specific investigations of the latest Pleistocene and early Holocene stratigraphy in Rose Valley and Indian Wells Valley, their study does not include geomorphic map data at resolutions needed for cultural resource management across NAWS China Lake.

4.0 SITE DESCRIPTION

China Lake basin is located in the northern Mojave Desert on the eastern side of the Sierra Nevada within Indian Wells Valley north of the city of Ridgecrest, California (Figure 1) and specifically situated at the extreme southern boundary of the Great Basin Section of the Basin and Range physiographic province (Hunt, 1974; Stewart, 1978). China Lake basin lies within the Tropical/Subtropical Desert Division, American Semi-Desert Province Ecoregion (Bailey, 1996) and has an arid to semi-arid climate with a mean annual precipitation of less than 130 mm (measured at Ridgecrest).

China Lake is currently a dry to seasonally wet playa, but at times during the late Pleistocene (and possibly during the early Holocene), a large pluvial lake system occupied both China Lake basin and adjacent Searles Lake basin (Smith and Street-Perrott, 1983). During these extreme pluvial periods, China Lake overflowed into Searles Lake basin and at high lake levels both basins would become integrated into a single body of water. The China-Searles Lake system was one in a series of lakes that were connected by the paleo-Owens River. The paleo- Owens River was fed primarily by runoff from the Sierra Nevada that was transmitted to Owens Lake, then to China-Searles Lake, Panamint Lake, and to Death Valley during prolonged wet periods (Figure 1). The general boundary and history of this regional interconnected hydrologic system have been

documented through detailed studies of most of the individual basins (*e.g.*, Smith and Street-Perrott, 1983; Bacon *et al.*, 2006; Jayko *et al.*, 2008; Phillips, 2008; Smith 2009), although China Lake itself has received relatively little study until recently (*e.g.*, Meyer *et al.*, 2011). Although the nature and magnitude of river inputs between the basins is just beginning to be understood, it is likely that the paleo-hydrologic history of the paleo-Owens River and the interconnected lakes played a role in the distribution and activities of the earliest Americans (*e.g.*, Davis, 1978).

4.1 REGIONAL GEOLOGIC SETTING

The China Lake basin, located in Indian Wells Valley north of the city of Ridgecrest, California is bordered on the west by the Sierra Nevada, on the east by the Argus Range, on the north by the Coso Range, and on the south by the El Paso Mountains (Figure 1). China Lake basin is located in the southern Walker Lane, a broad zone of active transtensional faulting located to the east of the Sierra Nevada (Stewart, 1988; Wesnousky, 2005).

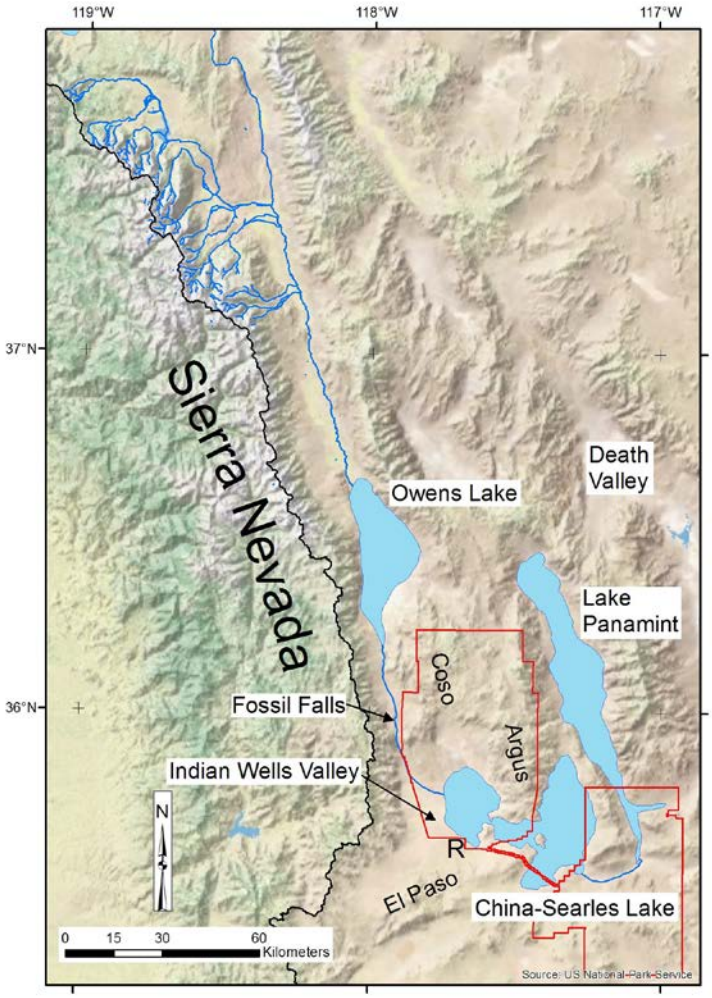

FIGURE 1. Map Showing Late Pleistocene Chain of Lakes Connected by Paleo-Owens River. The NAWS China Lake boundary is shown in red; R denotes the location of Ridgecrest.

Historical and Holocene active faults traverse the floor of Indian Wells Valley, which is also characterized by strong seismic activity (Figure 2). The north-trending, primarily right-slip, Little Lake fault zone (LLFZ) and the Airport Lake fault zone (ALFZ) traverse China Lake basin then diverge along the west and east flanks of the Coso Range volcanic complex. This broad, distributed zone of short, left-stepping, en echelon scarps has experienced two historical ground rupturing earthquakes, the first in 1982 (Roquemore and Zellmer, 1983) and the second in 1995 (Hauksson *et al.*, 1995). Although the surface rupture traces were relatively short (~2-3 km), they were associated with earthquakes of ML 4.9 and 5.4 (Hauksson *et al.*, 1995). The southern end of the 1872 rupture zone (M 7.6) of the Owens Valley fault is located about 75 km to the NNW of China Lake basin (Beanland and Clark, 1994). The Holocene active, left-lateral Garlock fault is located about 20 km south of China Lake basin (Figure 2).

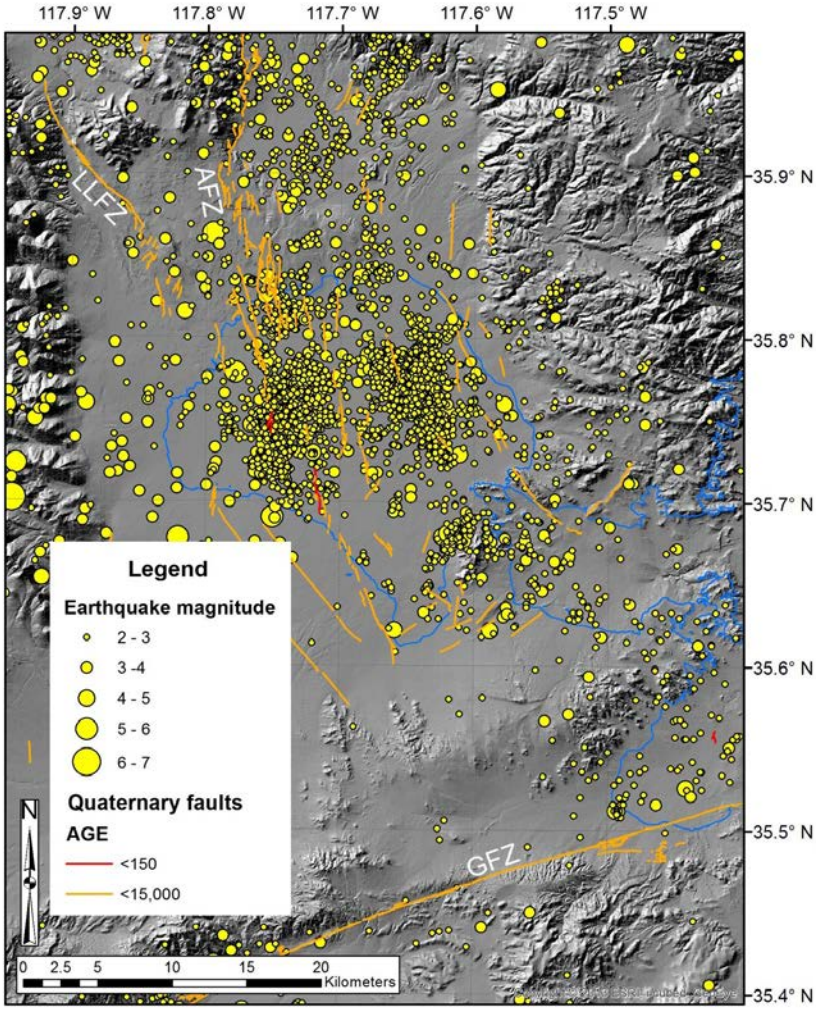

FIGURE 2. Map Showing Historical Seismicity and Location of Active Faults Within China Lake Basin Region (Southern California Earthquake Data Center). LLFZ = Little Lake fault zone, AFZ = Airport Lake fault zone, GFZ = Garlock fault zone. Late Pleistocene highstand of China-Searles Lake at 690 m is shown by the blue line.

Left stepovers in the right-slip LLFZ and ALFZ have resulted in complex surface deformation consisting of localized areas of small uplifted blocks and adjacent tectonic depressions. This style of deformation has influenced both the distribution of geomorphic units and their surface characteristics (*e.g.*, relative degrees of dissection) in China Lake basin below the 700 m contour.

4.2 GEOMORPHIC SETTING OF CHINA LAKE BASIN

China Lake basin represents the terminus for numerous streams that converge on Indian Wells Valley. The basin consists of a low-relief, irregular shaped playa covering about 20 km^2 surrounded by adjacent piedmonts comprised of alluvial fans, and abundant evidence of modification by lacustrine processes. Most of the playa surface is dissected by numerous dendritic channels, extending from the margins toward the center of the playa. Only a small part of the playa (~7 km^2), which consists of a planar horizontal surface is the current site of active ponding and deposition of fine-grained sediment and evaporates (Adams *et al.*, 2012a).

China Lake basin has long been thought to be a shallow arm of the much larger Searles Lake basin (Gale, 1914; Blackwelder, 1933) and the site where water first ponded before flowing over a low divide (sill) at an elevation of ~665 m. Upon reaching the 665 m sill, water in China Lake would then flow downstream between the south end of the Argus Range and Lone Butte, into the subbasin of Salt Wells Valley, and through Poison Canyon before entering Searles Lake basin (Plate B-1). When lake levels in Searles Lake rose above 658-665 m, both China and Searles basins integrated to form a single lake (*e.g.*, Smith, 1968; Smith and Street-Perrot, 1983; Phillips, 2008; Smith, 2009; Meyer *et al.*, 2011).

Evidence of former lake levels is readily observed at China Lake. Preserved shorelines in China Lake basin consist of isolated beaches, beach ridges, spits, and tombolos, as well as wave-cut escarpments developed on both unconsolidated sediments and on the flanks of bedrock knolls (Meyer *et al.*, 2011). These scattered shoreline remnants extend from an elevation of about 665 m up to the late Pleistocene highstand of about 690 m. In places, Meyer *et al.* (2011) noted well-developed shoreline remnants at 665 m, 670 m, 683 m, and 690 m; there is little age control on these features. Based on our geomorphic mapping, erosional shoreline remnants were also identified at elevations of 700-705 m. The age of the late Pleistocene highstand is poorly constrained by several tufa ages that range from about 11,870 to 12,970 ^{14}C yr B.P. (~13,700 to 15,000 cal yr B.P.) (Davis, 1978; Lin *et al.*, 1998; Smith, 2009). Although there is no direct age control on lower shorelines, the age of alluvial sediments sampled from a core drilled west of China Lake at an elevation of 669.6 m (Core 9 of Meyer *et al.*, 2011) suggests that China Lake had receded below an elevation of 665 m by about 9,690 ^{14}C yr B.P. (~10,800 - 11,230 cal yr B.P.).

Because of the previously described problems associated with dating tufa carbonate (Bischoff *et al.*, 1993), we directly dated sandy sediment with infrared stimulated luminescence (IRSL) analysis of sand grains (*e.g.*, Forman *et al.*, 2000). Results from luminescence analysis of duplicate samples we collected from a sandy deposit at an elevation of about 670 m near the China Lake outlet returned ages of latest Holocene. The age and sedimentology of the deposit sampled indicates the occurrence of mostly latest Holocene eolian sand accumulation that locally formed sand ramps in the area. In lieu of direct ages on the highstand shorelines in the lake basin, we assign the general ages to shorelines at 690 m and 683 m of ~14,550 ± 850 cal yr B.P. and a general constraining age for the 670 m shoreline between ~14,550 ± 850 and ~11,020 cal yr B.P.

In addition to shoreline features, there are abundant alluvial units in the China Lake basin that include distal alluvial fans derived from the Sierra Nevada, Argus Range, and El Paso Mountains, as well as flood debris fans and fragmented remnants of a fan delta complex that prograded into the China Lake basin. The flood debris fans represent sediment transport down the paleo-Owens River channel, possibly related to a large outburst flood(s) caused by sill failure at Owens Lake (Bacon *et al.*, 2014; see Appendix B). The fan delta is crossed by distributary channels along the path of the paleo-Owens River that are represented by an anastomosing network of channels with inset fluvial terraces and alluvial fans that grade to the playa of China Lake.

The degree of surface modification of the landscape has led to challenges in recognizing discrete landforms. Surface expression of geomorphic features in China Lake basin has been greatly modified by eolian erosional and depositional processes in the form of deflation hollows (blowouts) and expansive areas with active sand sheets and dunes, as well as areas of vegetated dunes and stabilized sand sheets with vegetation.

In addition to the detailed mapping performed below 700 m at China Lake, limited field studies upstream and downstream from China Lake have provided additional supporting evidence of large-scale flood events (*e.g.*, Amos *et al.*, 2013; Bacon *et al.*, 2014) that may have played a role of past large-scale flood events on the landscape history of the Owens-China- Searles lake system (see Appendix B).

5.0 GEOMORPHIC MAPPING METHODOLOGY

The geomorphic map combines sedimentologic characteristics (*e.g.*, alluvial deposits, lacustrine deposits, eolian deposits, etc.) with their associated landforms (*e.g.*, alluvial fans, beach ridges, sand dunes, etc.) to provide an integrated interpretation of landscape history. Landforms reflect the processes that shaped the landscape and commonly record subsequent erosional or depositional modification since the time they formed. For the purposes of this project, this type of map is treated as a geomorphic map that shows the distribution of landforms and features. The combined Phase I and II mapping encompasses the maximum areal extent occupied by China-Searles Lake when it reached its latest Pleistocene highstand of about 690 m (Figure 3). The Phase II map presented in this report has not been field checked because of test operations on the range that prevented access at the time fieldwork was conducted. Age determinations for sandy sediment associated with eolian sand ramps along the eastern playa margin near the outlet at an elevation of ~670 m have been included as an addendum to the previously issued report.

A field visit to both map areas was made between May 19 and 22, 2014 to evaluate the accuracy of imagery-based geomorphic mapping, as well as to make surface descriptions on identified geomorphic units and to assign relative geologic ages by verifying cross-cutting relations with identified and dated shorelines. Additional field visits were made March 17-21, 2014 and August 19-21, 2014 to areas surrounding NAWS China Lake to examine stratigraphic and geomorphic relations, as well as collect samples for age dating from key exposures to aid in deciphering the paleohydrologic history of China Lake.

5.1 TECHNICAL APPROACH

Mapping of landforms was carried out on high-resolution digital imagery and followed currently accepted surface geologic and geomorphic methods. Characteristic tonal and textural characteristics, such as differences in surface color, degree of dissection and channel network development, plus presence and density of vegetation (*e.g.*, Ray, 1960; Siegal and Gillespie, 1980; Bull, 1991) are qualitative indicators commonly used in the identification and delineation of discrete mapping units. Landforms were categorized into geomorphic units modified from classification schemes of Peterson (1981) and Bacon *et al.* (2010).

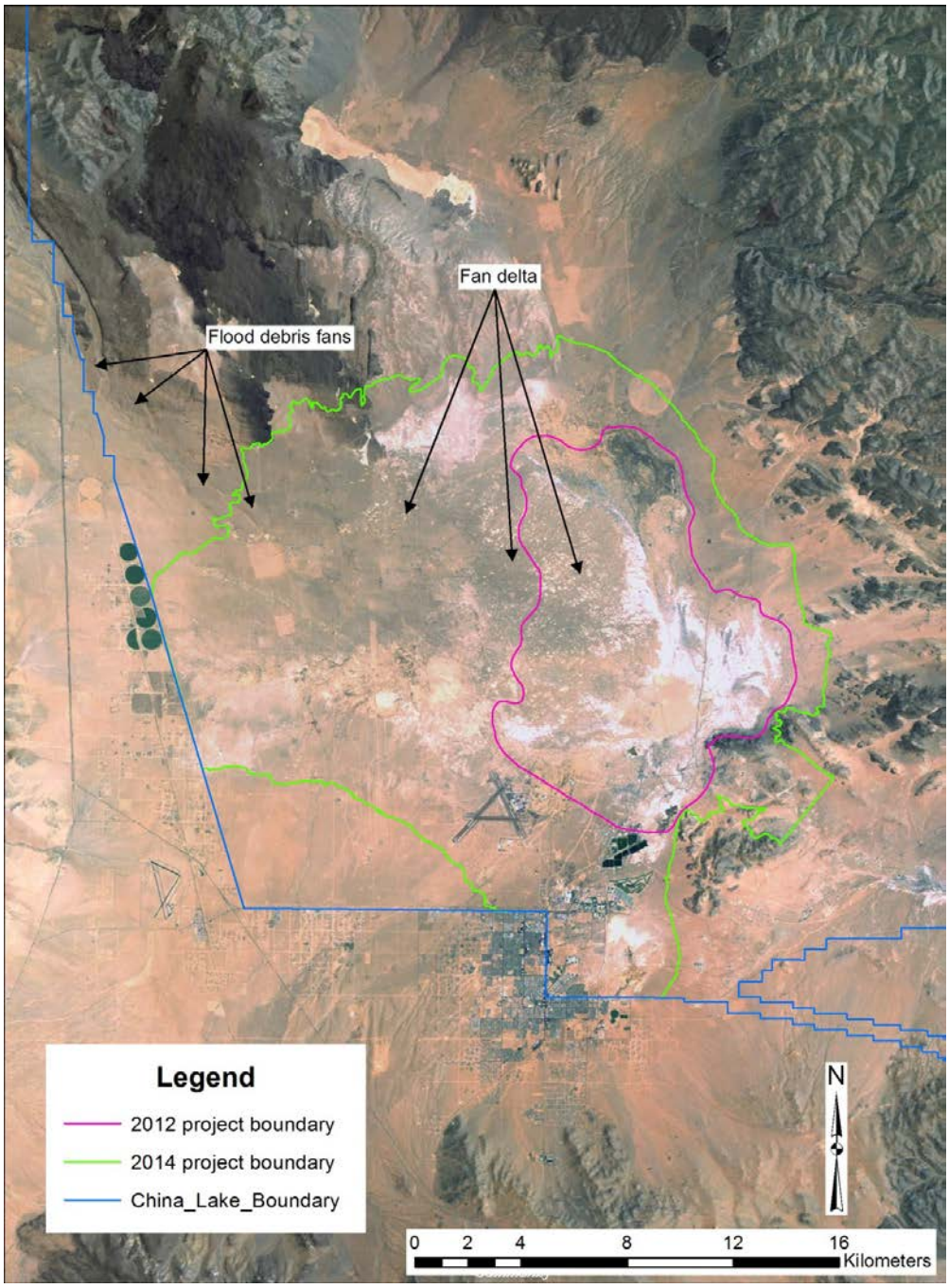

FIGURE 3. Map Showing Boundaries of 2014 (Phase II) and 2012 (Phase I) Map Areas. The general locations of flood debris fans and fan delta complex remnants are also shown.

As noted by House *et al.* (2013), the practice of geologic mapping is undergoing transformation in the way maps are made and used in order to meet the demands of modern map users and to accommodate future technological advances. Modern mapping and presentation has moved beyond pure field and office mapping on paper media to digital methods that are now being applied both in the office and in the field. We have adapted our mapping methods in the spirit of House *et al.* (2013) to produce a map that presents the components of the physical landscape at

China Lake within an intellectual and conceptual framework representative of the geomorphology at China Lake.

We performed our mapping using 1-meter USDA NAIP digital imagery, 10-meter digital elevation model, and 0.5-meter resolution imagery that was also used for spectral analysis in low-lying, low-relief areas. Map unit contacts and data were created in an ESRI ArcMap (v. 10) geodatabase. Google Earth was used in concert with digital mapping to provide imagery time series and elevation control. In an attempt to increase our mapping efficiency in areas characterized by thousands of small floodplain playas and playettes, we applied a digital mapping approach that takes advantage of spectral characteristics of imagery and the Principle Component tool contained in ArcGIS 10.0. The tool creates data layers consisting of lines that separate areas of specified spectral reflectance and allows the mapper to quickly attribute areas of high contrast reflectance (*e.g.*, Figure 4). Because the contrast in reflectance is generally low in piedmont areas, the Principal Component tool was not used to map alluvial fans or shoreline features on the piedmont.

5.2 ASSIGNMENT OF AGES TO LANDFORMS

Numerical ages for a few of the geomorphic units mapped for this effort are pending, but the relative ages of map units can be estimated using soil-geomorphic principles (*e.g.*, Birkeland, 1994) and cross-cutting relations between lacustrine (*i.e.*, shorelines) and subareal (*e.g.*, alluvial fans) features. By comparing characteristics of similar, dated landforms in areas adjacent to China Lake (*e.g.*, Owens Lake, Death Valley, Soda Lake and Silver Lake playas, Fort Irwin), using cross-cutting relations, and relying on professional experience conducting geomorphic studies in areas of the Mojave Desert adjacent to NAWS China Lake, we are able to constrain the age of most geomorphic surfaces to a period encompassing the latest Pleistocene and Holocene.

The age of most of the features on the floor of China Lake basin are younger than the latest Pleistocene highstand of China-Searles Lake, which is constrained to be between 13,700 and 15,000 cal yr B.P. based on the ages of tufa samples from the highstand shorelines (Davis, 1978; Lin et al., 1998; Smith, 2009). Bounding ages for the fan delta complex may be provided by radiocarbon-dated samples obtained from a core (Core 9 of Meyer et al., 2011) drilled on the south side of the fan delta complex adjacent to the western-central edge of China Lake basin. One sample was obtained from alluvial deposits at the top of lacustrine sand deposits (~11,120 cal yr B.P.) and the other from lacustrine silty sediments at the base of the core (~17,800 cal yr B.P.).

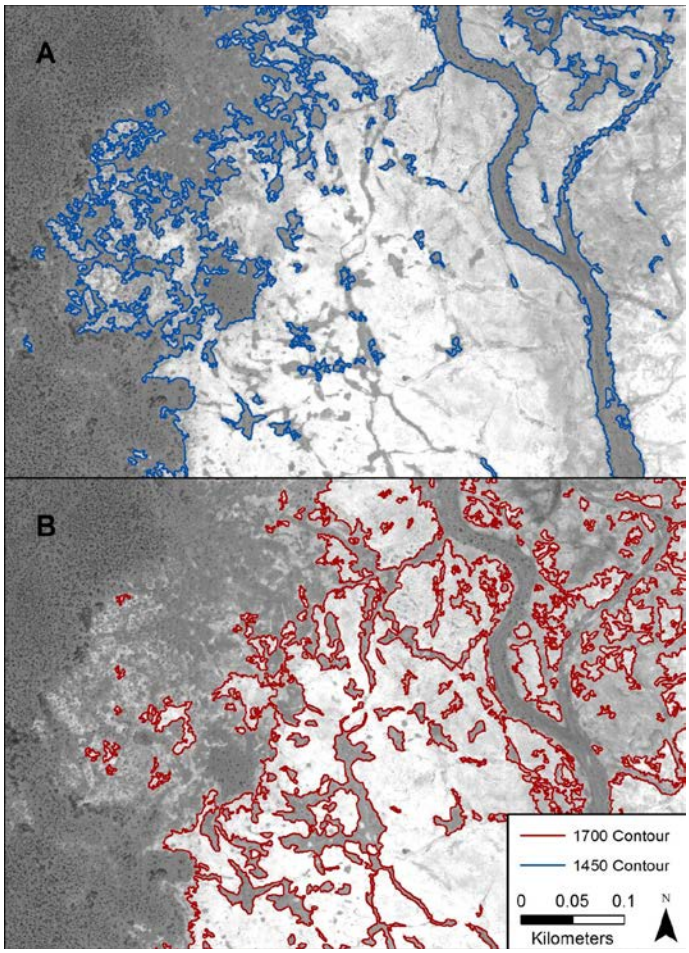

FIGURE 4. Two Examples Showing Level of Detail Associated With Application of Principle Component Analyses. (A) shows a 1450 PCA contour that delineates between a relatively dark surface and a surface with intermediate to high albedo (*i.e.*, light gray); (B) shows a 1700 PCA contour that has delineated only the high albedo surface. Mappers then managed the contours in an ArcGIS platform and assigned the groups into distinct geomorphic units.

To help refine the age of features on the floor of China Lake basin, samples were collected from sandy deposits at an elevation of about 669 to 670 m near the China Lake outlet for age determination (Figure 5). Samples were submitted to the Desert Research Institute E. L. Cord Luminescence Laboratory (DRILL) for analysis using infrared stimulated luminescence (IRSL) dating. The sample locale and elevation coincides with other sites at and near the same elevation (670 m) that contain constructional and erosional shoreline features, as well as the best developed and preserved shoreline features below the highstand shoreline at 690 m. Analysis of duplicate samples yielded ages of 1.61 ± 0.12 and 1.49 ± 0.11 ka and associated sedimentology indicate widespread eolian sand accumulation in the playa basin during the latest Holocene (Table 1). Future sample collecting is planned to help refine the age of landform features (e.g., 683 m, 690 m, and 700 m shoreline features, additional eolian features, and alluvial fans as appropriate) related to the paleohydrology of the basin.

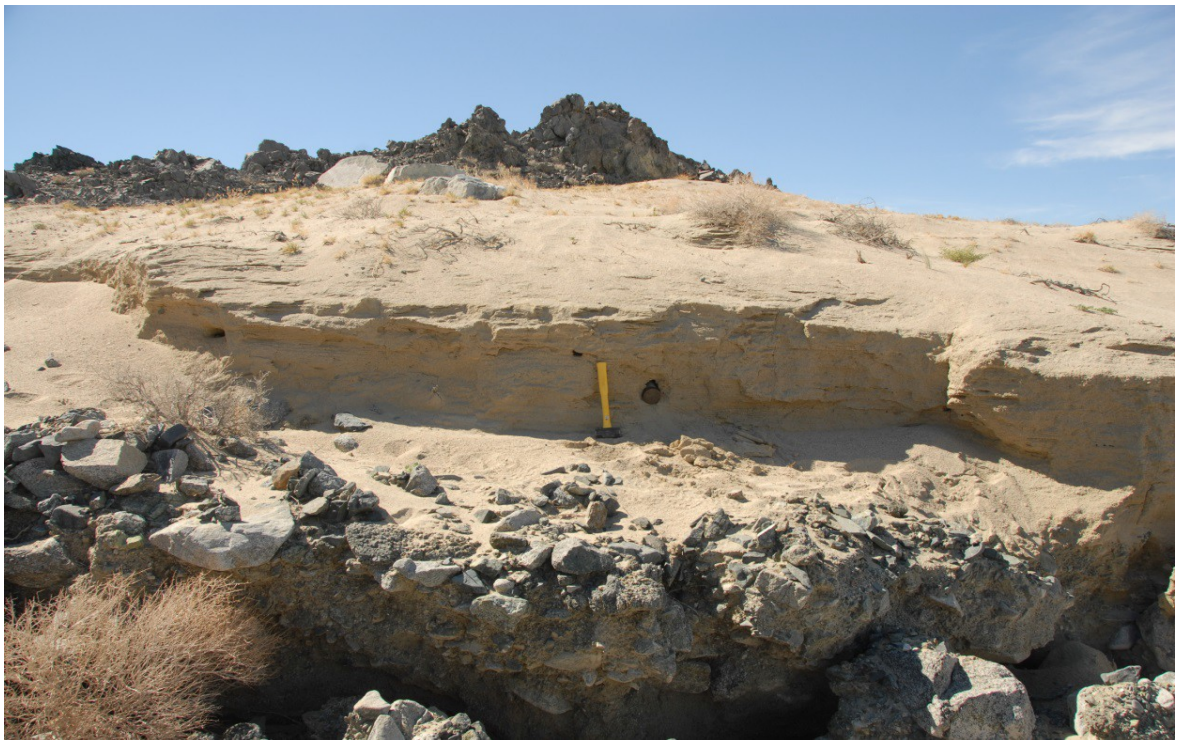

FIGURE 5. Photograph Showing a Natural Exposure Near China Lake Outlet at an Elevation of About 669 m. Samples for age analysis by infrared stimulated luminescence (IRSL) dating were collected from sandy eolian deposits adjacent to the sledge hammer.

To help with the broader paleohydrological context of the China Lake basin, additional IRSL samples were collected from the Owens Lake basin (Figure 1). A suite of five, well- developed, and well-preserved beach ridges in the southeastern part of Owens Lake basin were sampled at elevations of 1131 m, 1129 m, 1127 m, 1120 m, and 1114 m. These elevations represent times when Owens Lake last rose to the level of its natural sill and will provide temporal context for hydrologic connectivity between Owens Lake and China Lake. The IRSL samples were submitted to the UCLA luminescence laboratory for analysis and results will be presented in a peer-reviewed journal.

TABLE 1. Results of Single-Grain Post-IR IRSL Dating of Fine Sand Deposits Within an Eolian Sand Ramp Feature in China Lake Basin.

Sample number	Depth (m)	Location (decimal degrees)	Altitude (m)	N accepted (N analyzed)[a]	Over-dispersion (%)	D_b (Gy)[b]	U (ppm)[c]	Th (ppm)[c]	K (%)[c]	External beta dose rate wet (Gy/ka)	External gamma dose rate wet (Gy/ka)	Cosmic dose rate (Gy/ka)[d]	Total dose rate (Gy/ka)[e]	Age (ka)[f]
CL14-01	1.0	35.707 °N; 117.604 °E	668.95	80 (700)	29	6.6 ± 0.25	1.50	4.30	3.41	2.68	1.20	0.21	4.09 ± 0.26	1.61 ± 0.12
CL14-02	1.0			78 (700)	25	6.42 ± 0.22	1.31	6.77	3.50	2.77	1.32	0.21	4.30 ± 0.27	1.49 ± 0.11

[a] n is the number of D_e determinations accepted after screening; in parentheses are the total number of aliquots measured.

[b] The error shown on the burial dose, D_b, is the error modeled with the central age model (CAM) (Galbraith et al., 1999).

[c] U and Th samples were fused with lithium borate and measured with ICP-MS. K2O was measured on bulk sample with ICP-AES and converted to % K.

[d] Cosmic dose rates (Gy/ka) are calculated according to Prescott and Hutton (1994).

[e] Dose rates (Gy/ka) were calculated using the conversion factors of Liritzis et al. 2013 and are shown rounded to two decimal places; ages were calculated using values prior to rounding; central values are given for dose-rates and errors are incorporated into that given for the total dose-rate. Water content of 2% ± 1% was used for all dose rate calculations.

[f] Luminescence ages were calculated using DRACv1.2 (Durcan et al., 2015) and are expressed as thousands of years before 2015 and rounded to the nearest year. Error is 1 sigma.

References:

Durcan, J.A., King, G.E., and Duller, G.A.T., 2015. DRAC: Dose rate and age calculator for trapped charge dating. Quaternary Geochronology,

Galbraith, R.F., Roberts, R.G., Laslett, G.M., Yoshida, H., Olley, J.M., 1999. Optical dating of single grains of quartz from Jinmium rock shelter, northern Australia. Part I: experimental design and statistical models. Archaeometry, 41, pp. 339-364.

Liritzis, I., Stamoulis, K., Papachristodoulou, C., Ioannides, K., 2013. A re-evaluation of radiation dose-rate conversion factors. Mediterranean Archaeology and Archaeometry 13, 1-15.

Prescott, J.R., & Hutton, J.T. (1994). Cosmic ray contributions to dose rates for luminescence and ESR dating: large depths and long-term time variations. Radiation Measurements, 23, 497-500.

In lieu of numerical dates, landform surface characteristics, such as magnitude of bar- and-swale microtopography and the position of landform surfaces in relation to active channels (*i.e.*, degree of dissection and relief), as well as degree of desert pavement (*i.e.*, surface gravel density) and desert varnish (*i.e.*, dark, manganese oxide coatings) development were used to differentiate younger landforms from older ones (*e.g.*, McFadden *et al.*, 1989). Documenting these types of surface features and weathering characteristics in combination with using the few existing ages of shorelines from published studies (*e.g.*, Davis, 1978; Lin *et al.*, 1998; Smith, 2009; Meyer *et al.*, 2011) enabled the separation of primary geomorphic feature types into distinct landform units with an associated age class.

6.0 GEOMORPHIC MAP BELOW THE 700 M CONTOUR

The Phase II map area is comprised of many of the same low-gradient, basin floor geomorphic units previously mapped during Phase I. Because of the higher relief in Phase II map area between 665 m and 700 m elevation, a more diverse range of surface ages and landform feature types is present in the Phase II map area than in the Phase I map area below 665 m. Some of the older landform features identified around 700 m are the product of both internal and external paleohydrologic events (*i.e.*, lake-level fluctuations and large floods) that have influenced the landscape history of China Lake basin. Because of these observations, key areas above the 700 m contour were investigated to provide a larger areal and interbasin context of the geomorphology identified in China Lake basin (see Appendix B). The geomorphic map of China Lake basin below 700 m contour is presented in Plate 1 and is available as an ArcGIS geodatabase.

6.1 GEOMORPHIC MAP UNITS

Nine primary landform feature types were identified in the study including: hillslope, alluvial fan, deltaic, eolian, fluvial, lacustrine, playa, bedrock, and anthropogenic (Figure 6). These primary feature types were further separated into forty-eight distinct geomorphic units with their corresponding surface age when applicable (Table 2). Abbreviated descriptors for Quaternary feature types (*e.g.*, Qfl, fluvial; Qf, alluvial fan; Qdp, delta plain) were numbered from low to high numbers (*e.g.*, Qf1 to Qf5) on maps and tables, representing oldest to youngest geomorphic surfaces, respectively.

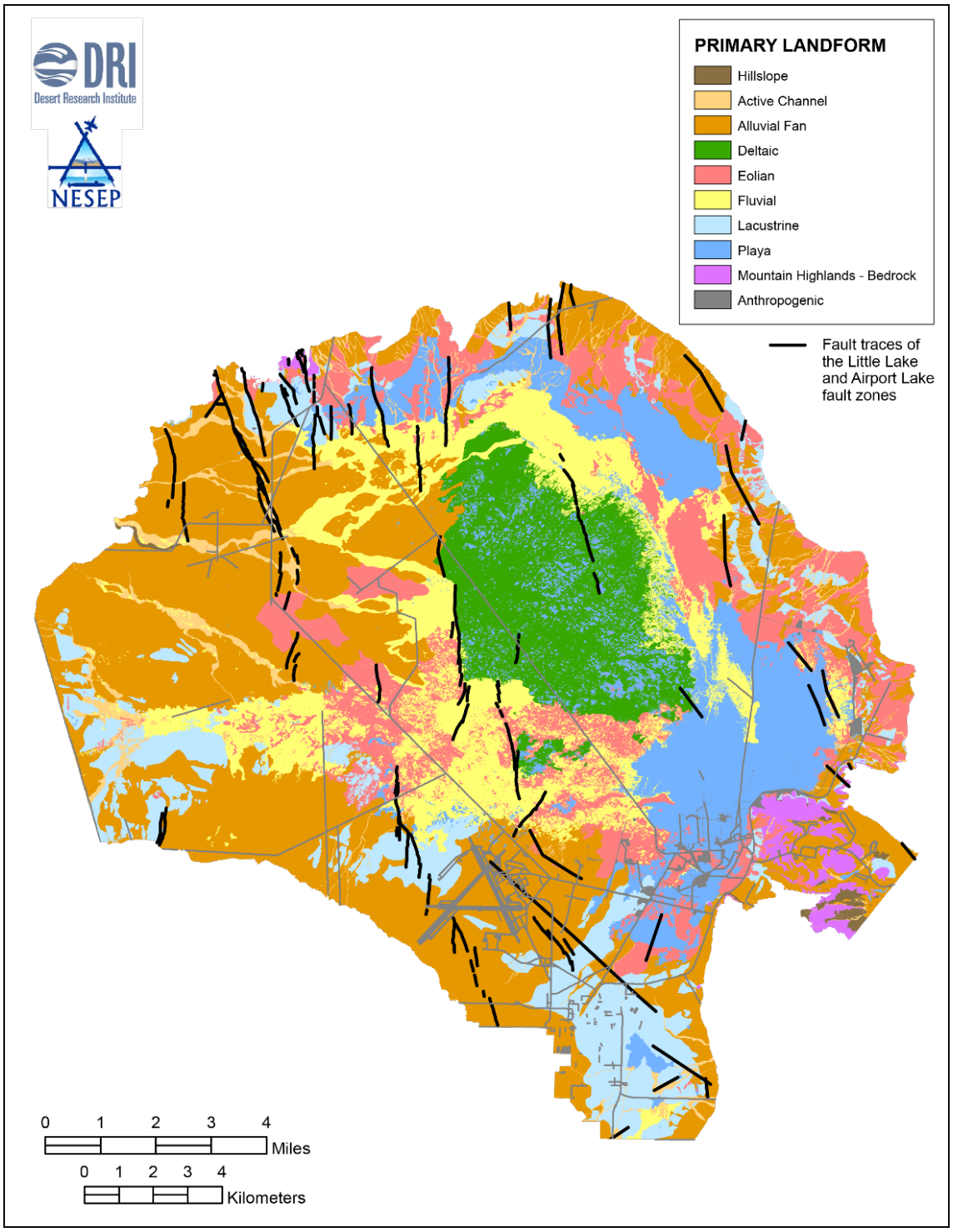

FIGURE 6. Geomorphic Map Showing Distribution of Primary Landform Feature Types. See Plate 1 for the detailed map that shows the 48 distinct geomorphic units.

Hillslope features were mapped as colluvial slopes [Qc] on steep bedrock slopes mostly within the eastern sector of the map and along incised channel walls of the paleo-Owens River in the western part of the mapped area.

Deltaic features were separated into an old delta plain [Qdp1] unit and an incised and young delta plain [Qdp2] unit. Both deltaic features occur below the 670 m shoreline and collectively form a fan delta complex with alluvial fan [Qf3] unit.

Eolian features [Qe] were differentiated into five distinct geomorphic units including: active sand dunes [Qe(d)], active sand sheets [Qe(ss)], inactive sand sheets [Qe(iss)], sand sheets with vegetation [Qe(ssv)], and vegetated sand dunes [Qe(vd)]. All five eolian geomorphic units extend across the map area with most occurring on the basin floor, as well as on piedmont slopes in the eastern part of the map area.

Alluvial features [Qf] were separated into eight distinct geomorphic units. These units include active channels [Qac], young alluvial fans [Qf5 and Qf4], intermediate-age alluvial fans [Qf3 and Qf2], and old alluvial fans [Qf1]. The Qf1 unit was further subdivided into surfaces with groundwater deposits [Qf1(gwd)] and into debris flood fan [Qf1(df3)]. The Qf1(df3) unit is the youngest debris flood fan of the paleo-Owens River that extends into the map area. See Appendix B for details of a suite of debris flood fans above the 700 m contour and their potential paleohydrologic significance to the map area. The Qf1, Qf2, and Qf3 units show geomorphic evidence of shoreline erosion and/or modification by the 690, 683, and 670 m lake levels, respectively. The relatively younger Qf4 and Qf5 units are mapped as being inset to as well as burying the older Qf1 – Qf3 units. Qf4 and Qf5 do not show geomorphic evidence of shoreline erosion and/or modification by the 690, 683, and 670 m lake levels, and in many places bury shoreline features.

Fluvial features [Qfl] were separated into three distinct geomorphic units. These units include old fluvial plain [Qflp1] and young fluvial plain [Qflp2], as well as young fluvial plain playa [Qflp(p)]. The Qflp units collectively form a well-developed meander belt system at the base of alluvial fans that drains into China Lake playa. The Qflp(p) unit mostly occurs within the margins of Qflp2 as isolated to broad areas frequently inundated by flooding, but also occurs in areas that have eolian features.

Lacustrine features [Ql] and beach features [Qb] were separated into seventeen distinct geomorphic units that represent three different lake environments and corresponding geomorphic surface ages. The different lake environments include beach platform [Qbpf], beach plain [Qbp], beach ridge [Qbr], and lake plain [Qlp] units. The beach and lake plain units were further divided into dissected beach plain [Qbp(d)] and dissected lake plain [Qlp(d)] units where surfaces are crossed by active channels or exhibit evidence of active erosion on relatively steeper slopes. The relative geomorphic surface ages of lacustrine and beach features at elevations of ~700, 690, 683, and 670 m were assigned numbers of 0, 1, 2, and 3, respectively.

Playa features [Qpl] on the floor of China Lake are parts of the basin-floor geomorphic environment characterized by broad and planar surfaces largely devoid of vegetation and occasionally flooded by ephemeral lakes. Other related types of features include playette [Qpl(pl)] (small playas), playa channels [Qpl(c)], dissected playas [Qpl(d)], playas subject to frequent inundation [Qpl(i)], playa margins [Qpl(m)], and seasonally inundated wetlands [Qw].

The remaining map units include bedrock outcrop composed of Quaternary volcanic rocks of basalt [Qv] and undifferentiated Mesozoic granitic rocks [Kg], as well as anthropogenic features including roads [An(r)] and other disturbed areas [An] (Table 2).

6.2 GEOMORPHIC UNITS BELOW 700 M CONTOUR

Landforms identified in the 390 km^2 study area exhibit a diverse range of surface and morphometric characteristics. Mapping shows that 59.2 percent of the area consists of landforms younger than early Holocene, of which 11.1 percent range in age from 8,200 to 4,200 cal yr B.P. and are associated with the young alluvial fans [Qf4]. The remaining 47.9 percent range in age from 4,200 to 2014 A.D. and consist of hillslope, alluvial, eolian, fluvial, and playa feature types (Table 2; Plate 1). The other 40.8 percent of the area consist of landforms that have an age of 15,000 – 13,700 yr cal B.P. (14,550 ±850 cal yr B.P.), which consist of intermediate and old alluvial fans, lacustrine, and deltaic feature types.

The three most prevalent landform feature types by areal extent in the map area are alluvial fan (37.3%), eolian (13.9%), and fluvial (13.1%) with the remaining feature types comprising of playa (12.1%), deltaic (9.3%), lacustrine (11.4%), and bedrock (1.3%), plus anthropogenic (0.6%) and hillslope (0.3%) (Table 2). Mapping also shows that the two most widespread geomorphic units in each of their respective landform feature types include 11.1 percent young alluvial fan [Qf4] and 7.9 percent young fluvial plain [Qflp2], followed by 6.5 percent dissected playa [Qpl(d)], 6.3 percent eolian sand sheet with vegetation [Qe(ssv)], 5.2 percent delta plain [Qdp1], 3.1 percent dissected beach plain, 690 m [Qbp1(d)], 1.2 percent granitic rocks [Kg], 0.5 percent anthropogenically disturbed areas [An], and 0.2 percent colluvial slopes [Qc] (Table 2). Appendix A provides a concise description of each landform unit's geomorphic characteristics and age constraints.

TABLE 2. Summary of Preliminary Geomorphic Surface Ages and Area Distribution of Landform Map Units in China Lake Basin Below 700 m Elevation Contour.

Landform Map Unit	Landform & Elevation AMSL	Geomorphic Surface Age	Area					
			hectares	acres	km^2	mi^2	Landform (%)	Map area (%)
Hillslope Features								
Qc	Colluvial slopes	4,200 cal yr B.P. to 2014 A.D.	67.7	167.4	0.68	0.26	55.9	0.2
Qbd	Badlands below 690 m	14,550 ± 850 cal yr B.P. to 2014 A.D.	53.4	132.0	0.5	0.2	44.1	0.1
		Total	121.1	299.4	1.21	0.47	100.0	0.3
Alluvial Fan Features								
Qac	Active channel	1850 and 2014 A.D.	1357.4	3354.2	13.6	5.2	8.7	3.5
Qf5	Young alluvial fan	4,200 cal yr B.P. to 2014 A.D.	1470.0	3632.4	14.7	5.7	9.6	1.5
Qf4	Young alluvial fan	8,200 and 4,200 cal yr B.P.	4346.9	10741.3	43.5	16.8	28.2	11.1
Qf3	Intermediate alluvial fan	14,550 ± 850 cal yr B.P.	4012.3	9914.6	40.1	15.5	26.1	10.3
Qf2	Intermediate alluvial fan	14,550 ± 850 cal yr B.P.	2604.6	6436.1	26.0	10.1	17.0	6.7
Qf1	Old alluvial fan	>14,550 ± 850 cal yr B.P.	1349.8	3335.4	13.5	5.2	8.7	3.5
Qf1(df3)	Old Debris flood fan	62,000 to ≥14,550 ± 850 cal yr B.P.	262.3	648.2	2.6	1.0	1.7	0.7
		Total	15,403.3	38,062.2	154.0	59.5	100.0	37.3
Deltaic Features								
Qdp2	Young delta plain	14,550 ± 850 to 11,020 cal yr B.P.	1607.4	3972.0	16.1	6.2	44.2	4.1
Qdp1	Old delta plain	14,550 ± 850 cal yr B.P.	2025.7	5005.5	20.3	7.8	55.8	5.2
		Total	3,633.1	8,977.5	36.3	14.0	100.0	9.3
Eolian Features								
Qe(d)	Eolian active dune	1850 and 2014 A.D.	238.4	589.2	2.4	0.9	4.4	0.6
Qe(ss)	Eolian active sand sheet	1850 and 2014 A.D.	2038.7	5037.7	20.4	7.9	37.6	5.2
Qe(iss)	Eolian inactive sand sheet	14,550 ± 850 to 4,200 cal yr B.P.	41.4	102.4	0.4	0.2	0.8	0.1
Qe(ssv)	Eolian sand sheet with vegetation	4,200 cal yr B.P. to 1850 A.D.	2449.8	6053.6	24.5	9.5	45.2	6.3
Qe(vd)	Eolian vegetated dune	4,200 cal yr B.P. to 1850 A.D.	653.5	1614.9	6.5	2.5	12.1	1.7
		Total	5,421.9	13,397.7	54.2	21.0	100.1	13.9

TABLE 2. Summary of Preliminary Geomorphic Surface Ages and Area Distribution of Landform Map Units in China Lake Basin Below 700 m Elevation Contour (Cont'd).

Landform Map Unit	Landform & Elevation AMSL	Geomorphic Surface Age	Area					
			hectares	acres	km^2	mi^2	Landform (%)	Map area (%)
Fluvial Features								
Qflp(p)	Young floodplain playa	1850 and 2014 A.D.	1477.6	3651.1	14.8	5.7	28.9	3.8
Qflp2	Young fluvial plain	1850 and 2014 A.D.	3082.0	7615.7	30.8	11.9	60.3	7.9
Qflp1	Old fluvial plain	4,200 cal yr B.P. to 2014 A.D.	555.2	1371.9	5.6	2.1	10.9	1.4
		Total	5,114.7	12,638.7	51.1	19.7	100.0	13.1
Lacustrine Features								
Qlp3	Lacustrine lake plain, 670 m	14,550 ± 850 cal yr B.P.	134.6	332.5	1.3	0.5	3.4	0.3
Qlp2(d)	Lacustrine dissected lake plain, 683 m	14,550 ± 850 cal yr B.P. to	434.8	1074.3	4.3	1.7	11.7	1.1
Qlp2	Lacustrine lake plain, 683 m	14,550 ± 850 cal yr B.P.	143.0	353.4	1.4	0.6	4.1	0.4
Qlp1-2	Lacustrine lake plain, 683 to 690 m	14,550 ± 850 cal yr B.P.	1.9	4.7	0.0	0.0	0.0	0.0
Qlp1(d)	Lacustrine dissected lake plain, 690 m	14,550 ± 850 cal yr B.P. to	460	1136.7	4.6	1.78	12.2	3.1
Qlp1	Lacustrine lake plain, 690 m	14,550 ± 850 cal yr B.P.	55.1	136.2	0.6	0.2	1.4	0.1
Qbr3	Lacustrine beach ridge, 670 m	14,550 ± 850 cal yr B.P.	0.6	1.6	0.0	0.0	0.0	0.0
Qbr1	Lacustrine beach ridge, 690 m	14,550 ± 850 cal yr B.P.	52.5	129.8	0.5	0.2	1.4	0.1
Qbp3	Lacustrine beach plain, 670 m	14,550 ± 850 cal yr B.P.	168.1	415.3	1.7	0.6	4.1	0.4
Qbp2(d)	Lacustrine dissected beach plain, 683 m	14,550 ± 850 cal yr B.P. to	16.0	39.6	0.2	0.1	0.7	0.0
Qbp2	Lacustrine beach plain, 683 m	14,550 ± 850 cal yr B.P.	612.5	1513.4	6.1	2.4	16.5	1.6
Qbp1(d)	Lacustrine dissected beach plain, 690 m	14,550 ± 850 cal yr B.P. to	816.1	2016.6	8.2	3.2	21.9	2.1
Qbp1	Lacustrine beach plain, 690 m	14,550 ± 850 cal yr B.P.	456.2	1127.3	4.6	1.8	12.3	1.2
Qbp1-3	Lacustrine beach plain, 670 to 690 m	14,550 ± 850 cal yr B.P.	2.9	7.1	0.0	0.0	0.0	0.0
Qbpf	Lacustrine beach platform below 690 m	14,550 ± 850 cal yr B.P.	322.4	796.6	3.2	1.2	8.2	0.8
	Lacustrine dissected beach							

TABLE 2. Summary of Preliminary Geomorphic Surface Ages and Area Distribution of Landform Map Units in China Lake Basin Below 700 m Elevation Contour (Cont'd).

Landform Map Unit	Landform & Elevation AMSL	Geomorphic Surface Age	Area					
			hectares	acres	km^2	mi^2	Landform (%)	Map area (%)
Qbp(o-d)	plain (old), above 690 m	>14,550 ± 850 cal yr B.P. to 2014 A.D.	12.1	29.8	0.1	0.0	0.0	0.0
Qbp(o)	Lacustrine beach plain (old), above 690 m	>14,550 ± 850 cal yr B.P.	82.6	204.2	0.8	0.3	2.1	0.2
		Total	3,771.4	8,9319.1	37.6	14.6	100.0	11.4
		Playa Features						
Qw	Seasonally inundated wetlands	1850 and 2014 A.D.	700.9	1732.0	7.0	2.7	14.9	1.8
Qpl(i)	Playa frequently inundated	1850 and 2014 A.D.	379.6	938.0	3.8	1.5	8.1	1.0
Qpl	Playa	1850 and 2014 A.D.	113.7	281.0	1.1	0.4	2.4	0.3
Qpl(pl)	Playette	1850 and 2014 A.D.	619.8	1531.6	6.2	2.4	13.2	1.6
Qpl(c)	Playa channel	1850 and 2014 A.D.	69.9	172.7	0.7	0.3	1.5	0.2
Qpl(d)	Dissected playa	4,200 cal yr B.P. to 2014 A.D.	2516.5	6218.4	25.2	9.7	53.5	6.5
Qpl(m)	Playa margin	4,200 cal yr B.P. to 2014 A.D.	303.9	751.0	3.0	1.2	6.5	0.8
		Total	4,704.4	11,624.8	47.0	18.2	100.0	12.1
		Anthropogenic Features						
An-r	Roads and cut or fill road bed	N/A	67.9	167.9	0.7	0.3	26.8	0.2
An	Anthropogenically disturbed areas	N/A	185.5	458.4	1.9	0.7	73.2	0.5
		Total	253.4	626.3	2.53	0.98	100.0	0.6
		Bedrock Features						
Qv	Quaternary basaltic rocks	N/A	40.1	99.2	0.4	0.2	7.9	0.1
Kg	Cretaceous granitic rocks	N/A	467.3	1154.8	4.7	1.8	92.1	1.2
		Total	507.5	1254.0	5.07	1.96	100	1.3
		Map Area Total	39,001.2	96,195.4	390.0	271.3	100.0	100.0

7.0 CONCLUSIONS AND FUTURE WORK

A detailed geomorphic map has been produced for the area of China Lake below the 700 m elevation contour (Plate 1). The map developed for this project has resulted in the most detailed geomorphic map currently available for the China Lake basin. Map unit data from all areas below the 700 m contour is integrated into a geomorphic geodatabase that can be searched and queried. We are now in a position to begin assessing the archaeological record in the context of chronologically discrete segments of the landscape. The map and geodatabase will allow us to correlate the distribution of known archaeological sites with landform types. This is a major step in our effort to create a geomorphic-based archaeological favorability model that relates the locations of archaeology to the landscape feature type and age and identifies areas favorable to containing archaeological materials. This will lead to a geomorphic-based tool that can provide cultural resource and installation managers with a method to strategize and assist decision making in terms of fiscal and human resource allocation, and ultimately to expedite access to testing and training areas. Detailed mapping of recognizable geomorphic features leads to an improved understanding of the complex latest Pleistocene and Holocene geomorphic history of China Lake basin. Despite the absence of numerical age control on the suites of landforms identified, using cross-cutting relationships, landscape position, and comparison with similar types of dated landforms in areas adjacent to China Lake, we have estimated ages of landscape assemblages to help us identify parts of the landscape having similar age, surface characteristics, and associated deposits, and to better understand surface process and responses under changing environmental conditions.

The geomorphic map will be an important tool that can be used for a number of different purposes in addition to its cultural resource application. These uses may include, but not limited to the assessment of natural hazards in China Lake basin, including flooding hazard, dust emission hazards, and areas susceptible to eolian sand transport, assessing geomorphic controls on the distribution of floral and faunal populations, and critical facilities siting. The geomorphic map also forms an important framework and basis for assessing potential landscape changes that may be associated with changing climate.

8.0 REFERENCES

Adams, K.D., and Wesnousky, S.G., 1998. Shoreline processes and the age of the Lake Lahontan highstand in the Jessup embayment, Nevada. Geological Society of America Bulletin 110, 1318-1332.

Adams, K.D., Bacon, S.N., Bullard, T.F., and Decker, D.L., 2012a. Preliminary geologic and geomorphic map of China Lake below 665 m, Inyo, Kern, and San Bernardino counties, California: Naval Earth Sciences and Engineering Program, Desert Research Institute, Publication no. 50002, 19 p.

Adams, K.D., Decker, D.L., and Bacon, S.N., 2012b. Review of the late Pleistocene to Holocene hydrologic history of China Lake, CA and surroundings: Naval Earth Sciences and Engineering Program, Desert Research Institute, Publication no. 50001, 19 p.

Aitken, M. J., 1998. Introduction to optical dating: Oxford, Oxford University Press, 256 p.

Altschul, J.H., Sebastian, L., and Heidelberg, K., 2004. Predictive modeling in the military – similar goals, divergent paths. SRI Foundation Preservation Research Series 1, 43 p.

Amos, C.B., Brownlee, S.J., Rood, D.H., Fisher, G.B., Burgmann, R., Renne, P.R., and Jayko, A.S., 2013. Chronology of tectonic, geomorphic, and volcanic interactions and the tempo of fault slip near Little Lake, California: Geological Society of America Bulletin, v. 125, p. 1187-1202.

Bacon, S.N., and Lancaster, N., 2012. Geomorphic Mapping of the Keeler Dunefield and Surrounding Areas. Final report prepared by Desert Research Institute for Great Basin Unified Air Pollution Control District, November 14, 2012, 63 p. including appendices and maps.

Bacon, S.N., Burke, R.M., Pezzopane, S.K., and Jayko, A.S., 2006. Last glacial maximum and Holocene lake levels of Owens Lake, eastern California, USA: Quaternary Science Reviews, v. 25, no. 11-12, p. 1264-1282.

Bacon, S.N., McDonald, E.V., Caldwell, T.G., and Dalldorf, G.K., 2010. Timing and distribution of alluvial fan sedimentation in response to strengthening of late Holocene ENSO variability in the Sonoran Desert, southwestern Arizona, USA. Quaternary Research, v. 73, p. 425-438.

Bacon, S.N., Adams, K.D., Bullard, T.F., Keen-Zebert, A., and Decker, D.L., 2014. Sill failure and catastrophic outburst floods from Owens Lake, California: Implications for latest Pleistocene and Holocene paleohydrology of the Owens River drainage basin: Geological Society of America Abstracts with Programs, v. 46, no. 6, p. 746.

Bailey, R.G., 1996. Description of ecoregions of the United States, 2nd edition: USDA-Forest Service Miscellaneous Publication 1391, Washington, D.C., 108 p.

Baker, V.R., 2009. The Channeled Scabland—A retrospective: Annual Reviews of Earth and Planetary Sciences, v. 37, p. 6.1-6.19.

Beanland, S., and Clark, M.M., 1994. The Owens Valley fault zone, eastern California, and surface rupture associated with the 1872 earthquake: U. S. Geological Survey Bulletin 1982, 29 p.

Benn, D.I., Owen, L.A., Finkel, R.C., and Clemmens, S., 2006. Pleistocene lake outburst floods and fan formation along the eastern Sierra Nevada, California: implications for the interpretation of intermontane lacustrine records. Quaternary Science Reviews, v. 25 p. 2729–2748.

Bischoff, J.L., Stine, S., Rosenbauer, R.J., Fitzpatrick, J.A., and Stafford Jr., T.W., 1993. Ikaite precipitation by mixing of shoreline springs and lake water, Mono Lake, California, USA. Geochimica et Cosmochimica Acta, v. 57, p. 3855-3865.

Blackwelder, E., 1933. Lake Manly: an extinct lake of Death Valley: Geographical Review, v. 23, p. 464-471.

Blair, T.C., and Mcpherson, J.G., 2008. Quaternary sedimentology of the Rose Creek fan delta, Walker Lake, Nevada, USA, and implications to fan-delta facies models: Sedimentology, v. 55, p. 579-615.

Blair, T.C., and McPherson, J.G., 2009. Processes and forms of alluvial fans, in A.J. Parsons and A.D. Abrahams eds., Geomorphology of Desert Environments, 2nd ed., Springer Science+Business Media B.V., pp. 413–467.

Briuer, F., Brown, C., Gillespie, A., Limp, F., Trimble, M., and Richeson, L., 2000. Report proceedings: cultural resources management workshop, June 13-16, 2000, Patuxent River Naval Air Station, Lexington Park, MD. Project 00-101, DoD Strategic Environmental Research and Development Program and DoD Legacy Resource Management Program, 28p. + 4 appendices

Bull, W.B., 1991. Geomorphic Response to Climate Change. Oxford University Press, New York, p. 326.

Bullard, T.F., 2010. Geomorphic mapping in support of an archaeological predictive model, Marine Corps Ground Air Combat Center, 29 Palms, California. Technical Report to ASM Affiliates, 12 p. plus maps.

Bullard, T.F. and Bacon, S.N., 2010. Chapter 5: Geomorphological investigations at San Mateo Creek, *in* M. Becker and J. Daniels eds., Hidden Landforms: A geomorphological and archaeological study of the Sierra Training Area on Marine Corps Base Camp Pendleton, San Diego County, California. ASM Affiliates, 97 p.

Bullard, T.F., Bacon, S.N., and Green, H.L., 2015. Development and documentation of geomorphic characteristics in support of a cultural resources/archaeological favorability model for Death Valley National Park. Final Report to National Park Service, Great Rivers Cooperative Ecosystem Studies Unit Task Agreement No. P13AC000904 under Cooperative Agreement No. P13AC00763, 56 p.

Bullard, T.F., McDonald, E.V., Trammel, E.J., and Dalldorf, G.K., 2010. Development of a geomorphic-based archaeological sensitivity model for the U.S. Army Yuma Proving Ground, Arizona. Final Report to Environmental Sciences Division, Cultural Resources, U.S. Army Yuma Proving Ground, 36 p.

Bullard, T.F., McDonald, E.V., and Baker, S.V., 2009. Integration of new methods in soils and geomorphology applied to cultural resources management on military lands: Geoarchaeology Workshop Final Report, October 20-22, 2008, San Diego, CA. U.S. Army Research Office, Grant No. W911NF-08-1-0479, Proposal No. 54968-EVCF, 31 p.

Burbank, D.W., and Anderson, R.S., 2012. Tectonic geomorphology: Hoboken, NJ, Wiley-Blackwell, 454 p.

Cerling, T.E., 1990. Dating geomorphologic surfaces using cosmogenic ^{3}He: Quaternary Research, v. 33, p. 148-156.

Chadwick, O.A., Hendricks, D.M., and Nettleton, W.D., 1987. Silica in duric soils: I. A. depositional model. Soil Science Society of America Journal, v. 51, p. 975-982.

Davis, E.L., 1975. The “exposed archaeology” of China Lake, California. American Antiquity, v. 40, p. 39-53.

Davis, E.L., 1978. The ancient Californians: Rancholabrean hunters of the Mojave lakes country: Los Angeles, Natural History Museum of Los Angeles County, Science Series 29, p. 193.

Duffield, W.A., and Smith, G.I., 1978. Pleistocene history of volcanism and the Owens River near Little Lake, California: U.S. Geological Survey Journal of Research, v. 6, p. 395-408.

Duffield, W.A., and Bacon, C.R., 1981. Geologic map of the Coso volcanic field and adjacent areas: U.S. Geological Survey Miscellaneous Investigation Series Map I-1200, 1:50,000-scale.

Flach, K.W., Nettleton, W.D., Gile, L.H., and Cady, J.G., 1969. Pedocementation: induration by silica, carbonates, and sesquioxides in the Quaternary. Soil Science, v. 107, p. 442-453.

Forman, S.L., Pierson, J., and Leper, K., 2000. Luminescence geochronology, *in* Noller, J.S., Sowers, J.M., and Lettis, W.R., eds., Quaternary Geochronology, Methods and Applications. American Geophysical Union Reference Shelf 4, Washington, DC, p. 157-176.

Gale, H.S., 1914. Salines in the Owens, Searles, and Panamint basins, southeastern California: U.S. Geological Survey Bulletin 580-L, p. 251-323.

Grayson, D.K., 2011. The Great Basin, a natural prehistory: Berkeley, University of California Press, 418 p.

Hauksson, E., Hutton, K, Kanamori, H., Jones, L., Mori, J., Hough, S., and Roquemore, G. 1995. Preliminary report on the 1995 Ridgecrest earthquake sequence in eastern California: Seismological Research Letters, v.66, no. 6, p. 54– 60.

House, P.K., Clark, R., and Kopera, J., 2013. Overcoming the momentum of anachronism: American geologic mapping in a twenty-first-century world, *in* Baker, V.R., ed., Rethinking the Fabric of Geology. Geological Society of America Special Paper 502, p. 103-125.

Jayko, A.S., Forester, R.M., Kaufman, D.S., Phillips, F.M., Yount, J.C., McGeehin, J., and Mahan, S.A., 2008. Late Pleistocene lakes and wetlands, Panamint Valley, Inyo County, California, *in* Reheis, M.C., Hershler, R., and Miller, G.H., eds., Late Cenozoic Drainage History of the Southwestern Great Basin and Lower Colorado River Region: Geologic and Biotic Perspectives: Boulder, CO, Geological Society of America Special Paper 439, p. 151-184.

Jenkins, D.L., and nineteen others, 2012. Clovis age western stemmed projectile points and human coprolites at the Paisley Caves: Science, v. 337, p. 223-228.

Kunkel, F., and Chase, G.H., 1969. Geology and ground water in Indian Wells valley, California: U.S.G.S. Open-File report 69-329, 84 p.

Lamb, M.P., Mackey, B.H., and Farley, K.A., 2014. Amphitheater-headed canyons formed by megaflooding at Malad Gorge, Idaho: PNAS, v. 111, p. 57-62.

Lancaster, N., 1995. The geomorphology of desert dunes. Routledge, London, 290 p. Lancaster, N., and Bacon, S.N., 2012. Late Holocene Stratigraphy and Chronology of Keeler Dunes Area. Final report prepared by Desert Research Institute for Great Basin Unified Air Pollution Control District, November 13, 2012, 19 p.

Lancaster, N., Baker, S., Bacon, S., and McCarley-Holder, G., 2015. Owens Lake dune fields: composition, sources of sand, and transport pathways. Catena, http://dx.doi.org/10.1016/j.catena.2015.01.003.

Langford, R.P., 2000. Nabkha (coppice dune) fields of south-central New Mexico, U.S.A. Journal of Arid Environments, v.46, p. 25-41.

Limp, F., 2006. SERDP and ESTCP technologies for cultural resources detection. Legacy Resource Management Program, DoD Cultural Resources Workshop, July 11-13, 2006, Marriott Sea-Tac Airport Hotel, Seattle, WA.

Lin, J.C., Broecker, W.S., Hemming, S.R., Hajdas, I., Anderson, R.F., Smith, G.I., Kelley, M., and Bonani, G., 1998. A reassessment of U-Th and C-14 ages for late-glacial high-frequency hydrological events at Searles Lake, California: Quaternary Research, v. 49, p. 11-23.

Lione, B., 2007. DoD Cultural resources workshop: prioritizing cultural resources needs for a sound investment strategy. Department of Defense, 2007 Sustaining Military Readiness Conference, July 30th– August 3rd, Orlando, FL.

McDonald, E. and Bullard, T., 2003. Summary of soil-geomorphic variables for predicting the location of surface and buried cultural resource features, National Training Center and expansion areas: Technical Report to Land and Heritage Conservation Branch, U.S. Army Corps of Engineers, ERDC-CERL, Champaign, IL.

McDonald, E., Bullard, T., Britt, T., and Ruiz, M.O., 2004. Chapter 20: Development of an archeological predictive model for management of military lands, *in* Caldwell, D.R., Ehlen, J., and Harmon, R.S., eds., *Studies in Military Geology*, Dordrecht, Netherlands, Kluwer Academic Publishers, p. 259-270.

McFadden, L.D., Ritter, J.D., and Wells, S.G., 1989. Use of multiparameter relative-age methods for age estimation and correlation of alluvial fan surfaces on a desert piedmont, eastern Mojave Desert, California. Quaternary Research, v.32, p. 276-290.

Meyer, J., Rosenthal, J., Byrd, B.F., Young, D.C., 2011. Constructing a regional historical context for terminal Pleistocene/Early Holocene archaeology of the north-central Mojave Desert: Report to Department of Defense, Legacy Management Program, Project 07-349, Cooperative Agreement Contract No. W912DY-07-02-0042 (W31RY072277563).

Miller, D.M., Schmidt, K.M., Mahan, S.A., McGeehin, J.P., Owen, L.A., Barron, J.A., Lehmkuhl, F., and Lohrer, R., 2010. Holocene landscape response to seasonality of storms in the Mojave Desert: Quaternary International, v. 215, p. 45-61.

Nickling, W.G. and Wolfe, S.A., 1994. The morphology and origin of Nabkhas, region of Mopti, Mali, West Africa. Journal of Arid Environments, v 28, p. 13-30.

O'Conner, J.E., 1993. Hydrology, hydraulics, and geomorphology of the Bonneville flood: Geological Society of America Special Paper 247, 83 p.

O'Connor, J.E., and Webb, R.H.,1988. Hydraulic modeling for paleoflood analysis. In: Baker, V. R., Kochel, R.C., Patton, P.C. eds., Flood Geomorphology. Wiley, NY, pp. 403–420.

Pedley, H.M., 1990. Classification and environmental models of cool freshwater tufas. Sedimentary Geology, v. 68, p. 143–154.

Peterson, F.F., 1981. Landforms of the Basin and Range province: defined for soil surveys. Nevada agriculture experiment station, University of Nevada, Reno, Technical Bulletin 28, 52 p.

Phillips, F.M., 2008. Geological and hydrological history of the paleo-Owens River drainage since the late Miocene, Late Cenozoic Drainage History of the southwestern Great Basin and Lower Colorado River Region: Geologic and Biotic Perspectives, Geological Society of America Special Paper 439, p. 115-150.

Pigati, J.S., Rech, J.A., Quade, J., and Bright, J., 2014. Desert wetlands in the geologic record: Earth Science Reviews, v. 132, p. 67-81.

Rango, A., Chopping, M., Ritchie, J., Havstad, K., Kustas, W., and Schmugge, T., 2000. Morphological characteristics of shrub coppice dunes in desert grasslands of southern New Mexico derived from scanning LIDAR. Remote Sensing and Environment 74, 26-44.

Ray, R.G., 1960. Aerial photographs in geologic interpretation and mapping. U.S. Geological Survey Professional Paper 373, 230 p.

Reheis, M.C., Adams, K.D., Oviatt, C.G., and Bacon, S.N., 2014. Pluvial lakes in the Great Basin of the western United States: A view from the outcrop: Quaternary Science Reviews, v. 97, p. 33-57.

Roquemore, G., and Zellmer, J., 1983. Ground cracking associated with the 1982 Magnitude 5.2 Indian Wells Valley earthquake, California: Geology, v. 36, 197–200.

Ruiz, M.O., 2002. The development and testing of an archaeological predictive model for Fort Irwin, California. Technical Report to U.S. Army Corps of Engineers CERL, Champaign, IL, contract DACA42-02, Task Order No. T-0016.

Saint-Amand, P., 1987. Red Cinder Mountain and Fossil Falls, California, *in* Hill, M.L., ed., Cordilleran Section of the Geological Society of America, Volume Centennial Field Guide: Whittier, Geological Society of America, p. 143-144.

Siegal, B.S. and Gillespie, A.R., 1980. Remote sensing in geology. New York, John Wiley & Sons, 702 p.

Smith, G.I., 1968. Late Quaternary geologic and climatic history of Searles Lake, southeastern California, *in* Means of correlation of Quaternary successions, Proceedings of the VII Congress, International Association for Quaternary Research, p. 293-310.

Smith, G.I., 2009. Late Cenozoic geology and lacustrine history of Searles Valley, Inyo and San Bernardino counties, California, U.S. Geological Survey Professional Paper 1727, 115 p.

Smith, G.I., and Street-Perrott, F.A., 1983. Pluvial lakes of the Western United States, *in* Porter, S.C., ed., The late Pleistocene: Minneapolis, MN, United States, Univ. Minn. Press, p. 190-212.

Stewart, J.H., 1978. Basin-range structure in western North America: A review, *in* Smith, R.B., and Eaton, G.P., eds., Cenozoic Tectonics and Regional Geophysics of the Western Cordillera: Geological Society of America Memoir 152, p. 1-31.

Stewart, J.H., 1988. Tectonics of the Walker Lane Belt, western Great Basin Mesozoic and Cenozoic deformation in a zone of shear, *in* Ernst, W.G., ed., Metamorphism and Crustal Evolution of the Western US, Ruby Volume VII: Prentice Hall, Englewood Cliffs, NJ, p. 685-713.

Trumbore, S.E., 2000. Radiocarbon geochronology, *in* Noller, J.S., Sowers, J.M., Lettis, W.R. eds., Quaternary Geochronology, Methods and Applications. American Geophysical Union Reference Shelf 4, Washington, DC, p. 41-60.

Walker, M.J.C., Berkelhammer, M., Bjorck, S., Cwynar, L.C., Fisher, D.A., Long, A.J., Lowe, J.J., Newnham, R.M., Rasmussen, S.O., and Weiss, H., 2012. Formal subdivision of the Holocene Series/Epoch: a discussion paper by a Working Group of INTIMATE (Integration of ice-core, marine and terrestrial records) and the Subcommission on Quaternary Stratigraphy (International Commission on Stratigraphy): Journal of Quaternary Science, v. 27, no. 7, p. 649-659.

Waters, M.R., 1992. Principles of geoarchaeology. Tucson, University of Arizona Press, 399 p.

Wesnousky, S.G., 2005. Active faulting in the Walker Lane: Tectonics, v. 24, TC3009, doi:10.1029/2004TC001645.

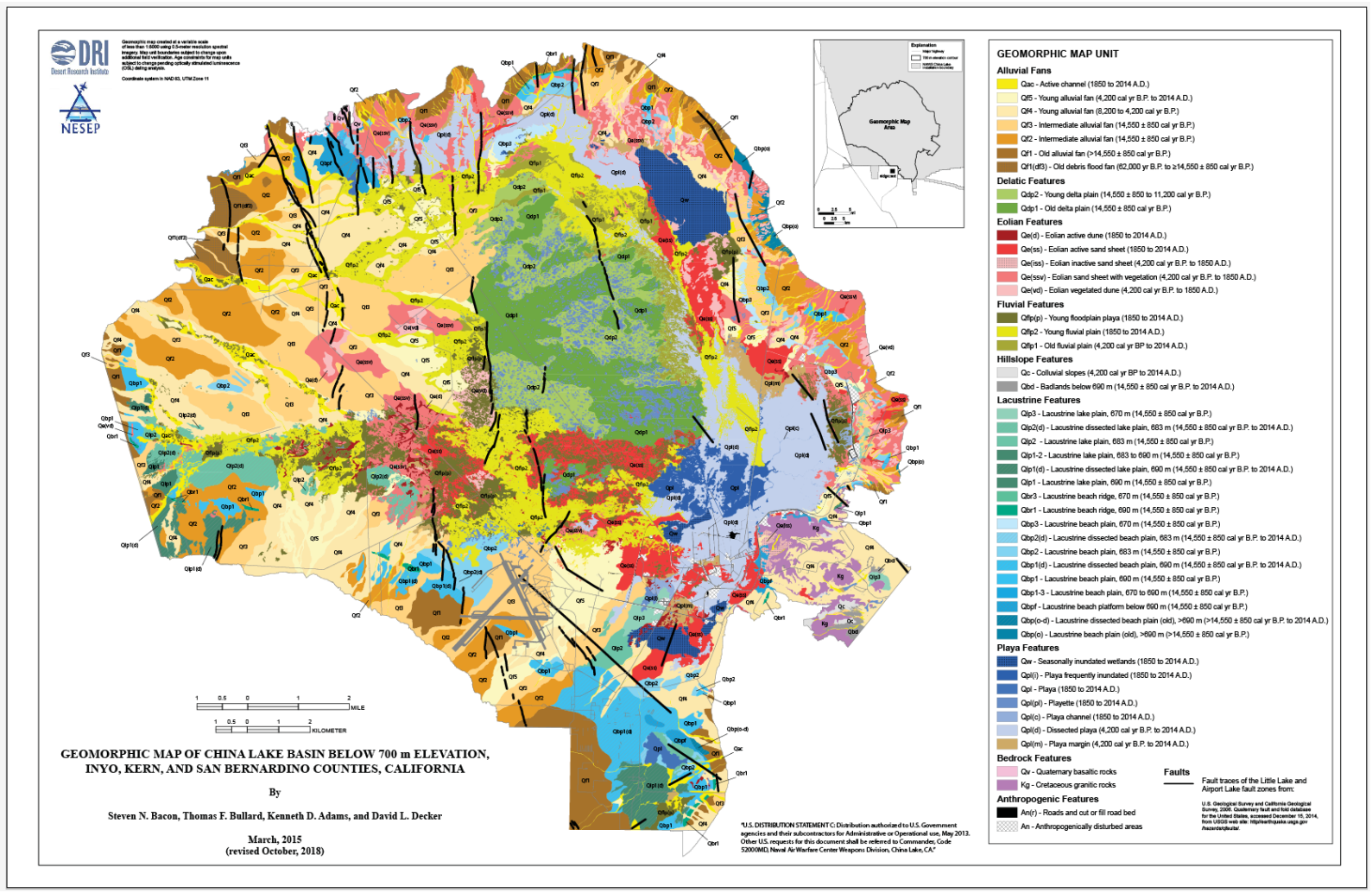

PLATE 1. Geomorphic Map of China Lake Basin Below 700 M Elevation, Inyo, Kern, and San Bernardino Counties, California.

Provided in electronic format as an attached file.
Filename: ***Plate_1_FINAL_Geomorphic_Map_China_Lake.pdf***
[Printing Instructions: File is formatted to print in a 34” x 22” size]

This page intentionally left blank.

Appendix A

GEOMORPHIC MAP UNIT DESCRIPTIONS

This page intentionally left blank.

Distribution Statement.

GEOMORPHIC MAP UNIT DESCRIPTIONS

The following unit descriptions detail the morphometric, surface, and shallow subsurface characteristics, as well as preliminary surface age constraints for each map unit identified in this study. Age constraints are considered preliminary until pending OSL luminescence analyses and additional fieldwork for this study are completed. Where applicable, published numerical ages from studies nearby in China-Searles basins and in the Mojave Desert region were used and correlated to provide preliminary age constraints of map units.

When specific ages were not available for a particular geomorphic unit, the age ranges outlined in Table A1 for epochs and sub-epochs are used following Grayson (2011) and Walker *et al.* (2012). The beginning of the historical period is hereby defined to be 1850 A.D.

Table A-1. General Age Ranges of Geomorphic Surfaces Used in This Study.

Time period	Calibrated age range
Historical	1850 – 2014 A.D.
Late Holocene	4.2 cal ka – 1850 A.D.
Middle Holocene	8.2 – 4.2 cal ka
Early Holocene	11.7 – 8.2 cal ka
Late Pleistocene	30 – 11.7 cal ka

HILLSLOPE UNITS [QC, QBD]

Two geomorphic feature types were identified in hillslope settings of the map area that include: colluvial slopes and badlands. Both feature types reflect relatively active erosion, transport, and deposition in moderately to steeply sloping and mostly unvegetated terrain.

Colluvial slopes [Qc]: This unit comprises 0.2 percent of the map area and includes thin to thick accumulations of coarse-grained deposits associated with recent deposition on or at the toe of steep to precipitous hillslopes associated with mountain highlands, hills, buttes, and incised channels. Due to the unit's geomorphic position on relatively steep slopes and young surface morphology, the Qc unit is assigned a late Holocene to historical age; Qc is constrained between ~4,200 cal yr B.P. and 2014 A.D.

Badlands (Qbd): This unit comprises 0.1 percent of the map area and represents highly eroded fine-grained sedimentary rocks within the China Lake sill area in the eastern part of the map area below an elevation of 690 m. In terms of active erosion or deposition, badlands are relatively geologically stable landforms that are characterized by localized low- to moderate-gradient alluvial deposition of variable mixtures of silts and sands with lesser amounts of gravel

by fluvial processes within a network of mostly well-defined and deeply incised channels. The relatively planar and stable portions of the Qbd unit along interfluve ridges have a maximum age of latest Pleistocene because the unit's surface was last modified/eroded by a regressive 690 m lake-level. Due to the presence of relatively steep hillslopes associated with dissected channels, the Qbd unit has a minimum geomorphic surface age of historical. As a result, the Qbd unit is constrained between 14,550 ± 850 cal yr B.P. and 2014 A.D.

ALLUVIAL UNITS [QAC, QF5, QF4, QF3, QF2, QF1, QF1(GWD), Q1FDF3]

Alluvial fans [Qf] are typically cone-shaped landforms that originate at a point where mountain drainages exit mountain blocks, which commonly are bounded by zones of faulting. Alluvial fans spread across the piedmont in a semicircular form from the fan apex at the range front. Some fans have irregular shape due to a lack of accommodation space imposed by adjacent fans or other obstacles (*e.g.*, Blair and McPherson, 2009). Alluvial fans within Indian Wells Valley are derived from the Argus Range, the Black Mountain area, and parts of the southern Sierra Nevada (Figure 1). The piedmonts surrounding China Lake playa are comprised of coalescing alluvial fans that interfinger with eolian and playa sediments along the playa margins. A series of relatively small, short, and steep alluvial fans are also derived from granitic highlands at Lone Butte and other steep, granitic hills at the southwest end of the Argus Range. Alluvial active channels [Qac] are a common landform component of many of the alluvial fans surrounding China Lake playa that grade into fluvial plain [Qflp] units. Flood debris fans [Qfdf] are similar in plan form to alluvial fans [Qf], but are characterized by their coarse, boulder- covered surfaces, with clasts ranging in size up to several meters in diameter arranged in distributary bars and anastomosing channels. These types of fans are found in the northwestern part of Indian Wells Valley where the paleo-Owens River channel enters the basin. The Qf1 unit was further subdivided into surfaces overlain by groundwater discharge deposits [Qf1(gwd)].

Alluvial active channel [Qac]: This unit encompasses 3.5 percent of the map area and represents the courses of active, confined stream flow during runoff from snowmelt or precipitation events. Alluvial channels in the map area originate within the mountain ranges, on alluvial fan surfaces of various ages, that grade into fluvial environments. Alluvial channels are sites of erosion, transport, and deposition of sediments ultimately derived from the mountains. Alluvial channels also rework sediment temporarily stored along channels, from stable alluvial fans, and from lacustrine and eolian features. The floors of alluvial channels commonly display braid-bar morphology. Some alluvial channels grade onto the China Lake playa where they are mapped as playa channels [Qpl(c)]. The age of deposits found in alluvial channels are historical to recent and are too young to have recognizable soil development greater than very thin (<1-3 cm) a horizons. Therefore, the Qac unit is assigned an age between ~1850 and 2014 A.D.

Young alluvial fan [Qf5]: This unit comprises 1.5 percent of the map area and is the youngest alluvial fan feature mapped in the area. The Qf5 unit is slightly incised by active distributary alluvial channels [Qac] and can be generally considered the active flood plain during large flood events where the unit is wide and gently sloping. The Qf5 unit typically grades to and extends across both young fluvial plain [Qflp2], playa margin [Qpl(m)], playa [Qpl] surfaces as continuous fan lobes. In the western part of the map area near active faulting the Qf5 unit is eroded and preserved as fan terraces within the margins of the Qflp2 unit and is positioned lower and inset to

the Qf4 unit. The Qf5 surface displays moderately- to well-developed bar-and-swale microtopography. Soils found on Qf5 unit are likely poorly-developed with surface clasts having little to no desert varnish similar to other documented young alluvial fans in the region (e.g., McFadden *et al.*, 1989). Unit Qf5 has no shoreline features developed on it. The absence of shoreline features, young surface morphology, and its close association with active channels and young fluvial plain and playa features, suggest that the Qf5 unit is late Holocene to historical in age. As a result, Qf5 is assigned an age between ~4,200 cal yr B.P. and 2014 A.D.

Young alluvial fan [Qf4]: This unit is the most prevalent geomorphic unit in the map area with an aerial distribution of 11.1 percent. The surfaces of the Qf4 unit are broad and gently sloping within the western and southwestern parts of the map area where they are incised into the distal parts of older fan units. In contrast, the Qf4 surfaces in the northern and eastern parts of the map area are relatively less extensive and more steeply sloping where derived from the Argus Range and the relatively low-relief hills and knobs near the China Lake basin sill area. The Qf4 unit has surface characteristics that range from muted to moderately developed bar-and-swale microtopography to surfaces that are relatively planar. Surfaces are underlain by variable mixtures of sand and gravel, and commonly covered by active sand sheets [Qe(ss)] and sand sheets with vegetation [Qe(vss)] at distal fan areas. Greater surface dissection and elevated landscape position relative to Qf5 surfaces indicates that Qf4 is relatively older. Although not observed in this study, soil on Qf4 would be expected to have a weak to moderately developed Bw to Bwkz horizon and detectable accumulation of secondary calcium carbonate and soluble salts similar too early to late Holocene fan soils in the Mojave Desert (e.g., McFadden *et al.*, 1989; McDonald, 1994; McDonald *et al.*, 2003; Miller *et al.*, 2010). Because the Qf4 unit is observed to either erode or bury the 690, 683, and 670 m shoreline features in many places, the unit is younger than the 670 m shoreline and is older than the Qf5 unit. Therefore, the Qf4 unit is constrained to an age between ~8,200 and ~4,200 cal yr B.P.

Intermediate Alluvial fan [Qf3]: This unit is the second most prevalent geomorphic unit in the map area with an aerial distribution of 10.3 percent. Surfaces of the Qf3 unit are broad and gently sloping within the western and southern parts of the map area where they are deeply incised into older [Qf1 and Qf2)] alluvial fans in areas near the mouth of the paleo-Owens River and the town of Ridgecrest. Similar to the Qf4 units, Qf3 surfaces in the northern and northeastern parts of the map area are relatively less extensive and more steeply sloping where they extend across older alluvial and lacustrine features. The Qf3 unit has surface characteristics that range from muted to moderately developed bar-and-swale microtopography to surfaces that are relatively planar and sand-rich where located downwind of areas covered by active and vegetated eolian feature types. Elevated landscape position relative to Qf4 surfaces indicates that the Qf3 unit is relatively older. Although not observed in this study, soil on the Qf3 unit would be expected to have a moderately developed Bwkz to Btkz horizon and detectable accumulation of secondary calcium carbonate and soluble salts similar too latest Pleistocene to early Holocene fan soils in the Mojave Desert (e.g., McFadden *et al.*, 1989; McDonald, 1994; McDonald *et al.*, 2003; Miller *et al.*, 2010). Because the Qf3 unit is observed to either erode or bury the 690 and 683 m shoreline features, but is graded to or eroded by the 670 m shoreline and deltaic features in many places, the unit is younger than the 690 and 683 m shoreline and is older than or time stratigraphic equivalent to the 670 m shoreline. As a result, the Qf3 unit is constrained to an age of 14,550 ± 850 cal yr B.P.

Intermediate Alluvial fan [Qf2]: This unit comprises 6.7 percent of the map area and is the second oldest alluvial fan unit mapped in the area. Where not covered by eolian sand deposits it is recognized on aerial imagery as relatively dark-colored surfaces that are moderately to deeply dissected by intermediate- and younger-aged alluvial fans. The Qf2 unit is present within most of China Lake basin, except in the sill area, as a continuous surface down to an elevation near 683 m where it has been truncated and eroded by past lake levels. The Qf2 unit exhibits muted surface channel microtopography and relic paleodistributary channels in the area of the paleo-Owens River and especially within areas downwind from identified eolian feature types in the northern and eastern sectors of the basin. A significant elevated landscape position relative to Qf3 surfaces indicates that the Qf2 unit is older. Although not observed in this study, soil developed on the Qf2 unit is expected to be similar to that developed on Qf3 surfaces. The age of this unit is younger than the 690 m highstand shoreline because the Qf2 unit erodes or buries the 690 m shoreline, but it is older than the 683 m shoreline because wave-cut notches and other lacustrine features truncate Qf2; the notches and truncations are evident as a prominent break-in-slope on 10-meter DEM. Therefore, the Qf2 unit is constrained to an age of 14,550 ± 850 cal yr B.P.

Old Alluvial fan [Qf1]: This unit comprises 3.5 percent of the map area and is the oldest alluvial fan unit mapped in the area. It is recognized on aerial imagery as relatively light-colored to dark- colored, deeply dissected erosional remnants of fans composed of variable mixtures of sand and gravel. The Qf1 unit typically occupies the highest topographic position on piedmonts, although in the eastern part of the mapping area it is observed to be flanked by, or partially buried by younger Qf2 and Qf3 alluvial fans. Although not observed in this study, soil developed on the Qf1 unit is likely to be complex because of surface erosion and/or burial by younger alluvial fans, but could be expected to have well-developed Bt and Btk horizons and accumulation of secondary calcium carbonate and silica similar to late Pleistocene fans in the region (e.g., Flach *et al.*, 1969; McFadden et al, 1989; Chadwick *et al.*, 1987; McDonald, 1994; McDonald *et al.*, 2003). The age of this unit is older than the 690 m highstand shoreline because the Qf1 unit is truncated by wave-cut notches and other lacustrine features formed at and near its lowest extent within the entire map area, except for the sill area, where no Qf1 fans were identified. Similar to the Qf2 unit, shoreline erosion across the Qf1 unit is evident as a prominent break-in-slope on 10-meter DEM. As a result, Qf1 is poorly constrained to older than 14,550 ± 850 cal yr B.P.

Old Flood debris fan [Qf1(df3)]: This unit comprises 0.7 percent of the map area and is the youngest flood debris fan unit. The unit occurs in the northwestern part of the mapping area above an elevation of 690 m. The Qf1(df3) unit occupies broad interfluves dissected (<5 m) by channels of the paleo-Owens River whose surfaces are largely covered by sand and fine gravel (Figure A1). In places, prominent distributary boulder bars composed of Qb2 and Qb3 basalt boulders (<2.5 m in diameter) and smaller granitic boulders (<1 m in diameter) are present on the surface (see Appendix B for details on Qb2 and Qb3 basaltic rock units and description of flood debris fans identified above the 700 m contour). Natural exposures in channel walls show the surface to be underlain by sandy gravelly boulder to bouldery gravel deposits. Phase II field observations indicate that the boulders in the Qf1(df3) unit become finer grained and less frequent downstream, but can still be traced to, but not below and across a prominent fault splay of the Little Lake fault zone at an elevation of the 690 m highstand shoreline. Until additional geomorphic data and direct numerical ages are collected, the age of the Qf1(df3) unit can be constrained to younger than the Qb3 basaltic rock unit and older than or the same age as the 690 m highstand shoreline. Therefore, the Qf1(df3) unit is poorly constrained between younger than ~62 ka and older than or equal to 14,550 ± 850 cal yr B.P.

FIGURE A-1. Large Basaltic and Granitic Boulders Lying on a Qfdf3 Unit at an Elevation of ~695 m Along Left Bank of One of Paleo-Owens River Channels In Northwestern Part of Map Area. Note the rock hammer (circled) in front of basalt boulder and the smaller granitic boulder to left.

DELTA PLAIN FEATURES [QDP1, QDP2]

The delta plain [Qdp] features identified in the map area represent the subaqueous facies of a large and broad fan delta complex formed due to alluvial fan deposition from the paleo- Owens River into standing water. Although many fan deltas are relatively steep (Blair and McPerson, 2008), the surface of the fan delta complex in the central part of the map area has low gradient slopes of about 0.0013 m/m that are crossed by a relic network of distributary channels and superabundant playette [Qpl(pl)] features within localized depressions. Two delta plain units were identified that delineate areas of primary deltaic deposition [Qdp1] and areas of significant erosion [Qdp2] from incision and reworking of primary depositional surfaces during lowering lake levels. The upslope extent of the Qdp units coincide with the 670 m elevation contour, as well as the distal extent of Qf3 alluvial fans, therefore the Qdp units are interpreted as the deltaic facies associated with the 670 m shoreline, and both units comprise the fan delta complex. The areal distribution of the delta plain units in the central part of the map area is strongly controlled by both active faulting along splays of the Little Lake and Airport Lake fault zones, as well as fluvial erosion as reflected by the extent of Qflp1 and Qflp2 units that encompass most of the Qdp units.

Young delta plain [Qdp2]: This unit comprises 4.1 percent of the map area and is the youngest delta plain unit. The Qdp2 unit is primarily composed of sand and has poorly-defined positive- relief distributary channels that are situated above the surrounding landscape. The Qdp2 unit is an erosional surface inset with the older Qdp1 unit and represents significant down-cutting due to changing base levels associated with a receding 670 m lake level. Most of the Qdp2 surface consists of both relic channel scars and thin sand sheets that have accumulated from the reworking of delta plain sediment by eolian processes. The Qdp2 unit is younger than Qdp1 unit and the 670 m shoreline based on its inset position with these units. Furthermore, the Qdp2 unit has a minimum age of ~11,020 cal yr B.P. from the maximum age of alluvial and aeolian sediments dated in Core 9 of Meyer *et al.* (2011). As a result, the Qdp2 unit is constrained in age to between 14,550 ± 850 and 11,020 cal yr B.P.

Old fan delta [Qdp1]: This unit comprises 5.2 percent of the map area and is the oldest delta plain unit. The Qdp1 unit is primarily composed of sand and has moderately to poorly defined positive-relief distributary channel features that are situated above the surrounding landscape. Many parts of the surface of this unit have been reworked by eolian processes into sand sheets and by scour from fluvial processes within its boundaries (*i.e.,* Qdp2) and in areas that surround it (*i.e.,* Qflp1 and Qflp2). On stable and relatively elevated surfaces of the unit, sand sheets have accumulated, but have not completely masked the morphology of Qdp1 channels. The Qdp1 unit is older than Qdp2 unit based on topographic and cross-cutting relations and is assigned a depositional age equivalent to the 670 m shoreline. As a result, the unit is constrained in age to about 14,550 ± 850 cal yr B.P.

EOLIAN FEATURES [QE(D), QE(VD), QE(SS), QE(ISS), QE(SSV)]

A wide range of eolian feature types were identified in the map area that include the following units: active sand dune [Qe(d)], vegetated sand dune [Qe(vd)], active sand sheet [Qe(ss)], inactive sand sheet [Qe(iss], and sand sheet with vegetation [Qe(vss)]. The formation and accumulation of large expanses of dunes and sand sheets are determined by the production of sediment in a range of suitable particle sizes, the availability of this sediment for transport by the wind, and the effective transport capacity of the wind (Lancaster, 1995). Most of the dunes and other types of accumulations of wind-blown sediment in the study area are derived from the sandy feature types of the map area, and in particular from the fluvial plain [Qflp], young alluvial fans [Qf], delta plain [Qdp], and playa [Qpl] feature types, as well as localized anthropogenically disturbed areas. Many of the dunes form distinct dune fields consisting of isolated areas with the Qe(d) and Qe(ss) units, plus a more extensive area composed of the Qe(vd) unit in places that are within or adjacent to low-gradient and broad fluvial plain and playa feature types. Most of the eolian features in the map area consist of a thin veneer of the Qe(ssv) unit or thicker accumulations in the form of large vegetated dune fields consisting of the Qe(vd) unit that bury alluvial fan and lacustrine feature types in the northern and eastern sectors of the basin. Isolated and less extensive Qe(iss) units are located downwind of playa feature types in the form of relic sand ramps that have been subsequently eroded and inset by younger alluvial fans along the base of low relief hills near the China Lake sill area.

Eolian active sand dunes [Qe(d)]: This unit comprises 0.6 percent of the map area. The Qe(d) unit includes areas of active sand transport and the accumulation of well-developed transverse dunes, small patches of transverse dunes, and parabolic dune forms, as well as sinuous dune forms resulting from the complex interactions of different dune forms, such as the coalescing of linear, transverse, and parabolic dunes. The Qe(d) landforms are commonly associated with, and sometimes overlie sand sheets [Qe(ssv)] and floodplain playas [Qfp(p)] and/or have accumulated with these feature types at a similar time, thereby having an inter-fingering stratigraphic relationship. The surfaces of the Qe(d) are mostly unvegetated and the site of active sand transport. The age of deposits found in the Qe(d) unit are historical to active because they lack recognizable soil development and exhibit contemporary activity. Therefore, the Qe(d) unit is assigned an age between ~1850 and 2014 A.D.

Eolian sand dunes with vegetation [Qe(vd)]: This unit comprises 1.7 percent of the map area. The Qe(vd) unit contains features with positive surface relief and moderate vegetation cover. This unit also includes patchy areas with transverse, parabolic, and sinuous dune forms that are stabilized by vegetation. The Qe(vd) unit commonly forms an assemblage with the sand sheet with vegetation [Qe(ssv)] unit that has been deposited on the distal parts of the youngest alluvial fans [Qf5 and Qf4] and flood plain [Qflp2] units. These dunes are mostly moderately vegetated, indicating that they are not presently geomorphically active, although, in localized areas it is common to see active sand sheets [Qe(ss)] within map boundaries (Figure A2). The Qe(vd) unit is constrained to late Holocene to historical in age because of its geomorphic position on top of the youngest alluvial fan and flood plain units in the map area. This age constraint is supported by workers in Owens Lake basin who mapped and dated similar vegetated dune features at ~1,700 yr B.P. to 1850 A.D. (Lancaster *et al.*, 2015; Bacon and Lancaster, 2012; Lancaster and Bacon, 2012). As a result, the Qe(vd) unit is constrained with a correlated age between about 4,200 cal yr B.P. and 1850 A.D.

Eolian active sand sheet [Qe(ss)]: This unit comprises 5.2 percent of the map area and consists of mobile accumulations of sand up to several meters thick that form flat surfaces with either low amplitude sand ripples less than 1 m in height that are devoid of vegetation or planar and smooth surfaces with sparse vegetation. The Qe(ss) unit is found on the margins of playa features and downwind of anthropogenically disturbed areas. In places it is difficult to distinguish the margins between Qe(ss) from vegetated sand sheets [Qe(ssv)] and young alluvial fans [Qf5 and Qf4] unit because they interfinger and form similar low-gradient, sand-rich surfaces. The Qe(ss) unit is constrained to historical to active because of the active eolian processes that influence its formation, as well as having similar morphometry and poor vegetation density to other sand sheet features mapped and dated in Owens Lake basin (Lancaster *et al.*, 2015; Bacon and Lancaster, 2012; Lancaster and Bacon, 2012). Therefore, the Qe(ss) unit is constrained with a correlated age between about 1850 A.D. and 2014 A.D.

Eolian inactive sand sheet [Qe(iss)]: This unit comprises 0.1 percent of the map area. The Qe(iss) unit is found on the flanks of Lone Butte and other granitic knobs and hills at the southern end of the Argus Range in the southeastern sector of the map area. The Qe(iss) unit is typically expressed as relatively thick (<5 m) accumulations of sand in the form of sand ramps on bedrock. Although there are probably zones within the Qe(iss) unit that display evidence of recent sand movement in the form of wind ripples or small dunes, the surface of this unit is currently being eroded by small alluvial channels [Qac] that are associated with young alluvial fans [Qf5], which have reworked, or bury, parts of Qe(iss). IRSL samples from the Qe(iss) unit yielded a late Holocene age of ~1.55 ka (see Table 1). Therefore, the Qe(iss) unit is poorly constrained in age to younger than 14,550 ± 850 cal yr B.P. and older than ~1850 A.D.

FIGURE A-2. Moderately Vegetated Parabolic Dune [Qe(vd)
Unit in West-Central Part of Mapping Area.

Eolian sand sheet with vegetation [Qe(ssv)]: This unit comprises 6.3 percent of the map area. The Qe(ssv) unit includes areas of inactive to active sand transport and deposition in areas with abundant vegetation; it is not characterized by coppice dunes but may contain areas of coppice dunes near the playa margin or other areas with relatively high groundwater. The difference between the Qe(ssv) unit and the active Qe(ss) unit is the degree to which they are covered by vegetation and relative geomorphic activity. The Qe(ssv) unit can be constrained to late Holocene to recent, because of its close association and apparent co-depositional relationship with the youngest alluvial fan [Qf5] in the map area. Qe(ssv) surfaces have similar morphometry and relative vegetation density to other vegetated sand sheet features mapped and dated in Owens Lake basin to be ~1,700 yr B.P. to 1850 A.D. (Lancaster *et al.*, 2015; Bacon and Lancaster, 2012; Lancaster and Bacon, 2012). Therefore, the Qe(ssv) unit is constrained with a correlated age between about 4,200 cal yr B.P. and 1850 A.D.

FLUVIAL FEATURES [QFLP(P), QFLP2, AND QFLP1]

Fluvial features and landforms are the result of erosion, transport, and deposition that occurs primarily in well-defined channels. Active channel migration in sinuous streams commonly results in the development of abandoned meanders and channel scars. In the north- central part of the map area, a series of two, identifiable meander belts consisting of older and younger fluvial plain surfaces [Qflp1 and Qflp2], respectively, display multiple channel remnants and meander scars on low-gradient slopes adjacent to the distal parts of alluvial fans. The fluvial plain landform represents the relatively unconfined flow sourced from alluvial fans across planar and low-gradient slopes. Surfaces are mostly underlain by sandy fluvial deposits, except in areas of recent ponding of fine-grained sediment from alluvial-fan flooding in the form of young fluvial floodplain playa [Qflp(p)]. The differences in relative age of the three fluvial plain landforms was determined by their cross-cutting relations with Qflp2 and Qflp(p) units being the youngest and lowest surfaces and Qflp1 being the oldest and highest fluvial unit.

Fluvial floodplain playa [Qflp(p)]: The floodplain playa unit comprises 3.8 percent of the map area and consists of relatively flat accumulations of sand and silt within drainage channels that were deposited by ephemeral stream flow (Peterson, 1981). They are recognized on imagery as small to large irregular areas of medium to high albedo within and adjacent to fluvial channels. Floodplain playas are typically unvegetated and display evidence of minor eolian reworking in the form of sand ripples and areas of coppice dunes along its edges. The Qflp(p) unit is commonly separated by low relief (<1m) transverse ridges of sand [Qe(ssv)] and form small interdunal playas between sand dunes [Qd(d)] and sand dunes with vegetation [Qe(vd)] units.

The Qflp(p) unit is commonly connected by shallow alluvial channels [Qac] that are highlighted by vegetation, compared to the surfaces of Qflp(p). Based on the unit's location in the bottom of ephemerally-active drainages of the younger Qflp2 unit and active eolian feature types, the age of Qflp(p) is constrained to between 1850 and 2014 A.D.

Young fluvial plain [Qflp2]: This unit comprises 7.9 percent of the map area and is the youngest fluvial plain unit. The Qflp2 surface is in the form of a meander belt with a network of braided and distributed active channels and channel scars filled with fluvially transported sand. The Qflp2 unit includes the Qflp(p) unit and is commonly covered by local to extensive

accumulations of a wide range of eolian feature types. Channel remnants of Qflp2 exhibit complex cross-cutting relations; however, the unit is inset to the older Qflp1 unit, and therefore is younger. Based on the unit forming the lowest surface, and potentially being an "active" geomorphic surface during flooding due to its connectivity with active channels [Qac] derived from distal alluvial fans, the age of the Qflp2 unit is constrained to between 1850 and 2014 A.D.

Old fluvial plain [Qflp1]: This unit comprises 1.4 percent of the map area and is the oldest fluvial plain unit. The Qflp1unit has similar surface characteristics to the younger Qflp2 unit, but is older based on cross-cutting relations and its higher landscape position relative to the younger flood plain unit. The Qflp1 unit is also younger than late Holocene to early Holocene alluvial fans [young Qf5 and intermediate Qf3] and both delta plain [Qdp] units in areas crossed by active faults, because the Qflp1 unit is either inset to or graded to these older units. As a result, the unit is poorly constrained between ~4,200 cal yr B.P. and 2014 A.D.

LACUSTRINE FEATURES [QBP(O), QBP(O-D), QBPF, QBP1-3, QBP1, QBP1(D), QBP2, QBP2(D), QBP3, QBR1, QBR3, QLP1, QLP1(D), QLP1-2, QLP2, QLP2(D), QLP3]

A wide variety of lacustrine landforms is found at a range of elevations between about 700, 690, 683, and 670 m in Indian Wells Valley that represents different processes and depositional environments associated with lake-level fluctuations of China-Searles Lake. At the margins of the former lake, beach ridges [Qbr] composed of linear accumulations of sand and gravel parallel to the shore were formed by the action of breaking waves (e.g., Adams and Wesnousky, 1998; Reheis *et al.*, 2014). Other shoreline features include small patches to linear accumulations of wave-affected, basinward-sloping sand and gravel surfaces in the form of beach plains [Qbp]. In places, lacustrine plains [Qlp] composed of gently sloping sand and gravel surfaces are found in front of, and downslope of the beach ridges and beach plains.

Erosional features are also present in the map area in the form of beach platforms [Qbpf] that represent the position of former lake levels. Evidence of former lake levels also includes wave cut/beveled surfaces across relatively steeply sloping old alluvial fans [Qf1 and Qf2] or volcanic [Qv] and granitic [Kg] bedrock. Also present is a subset of lacustrine features that are significantly dissected (d). These particular areas contain widely distributed rilling and channelization across mapped surfaces that appear to be the product of climatic- and/or tectonic- driven base-level changes.

Lacustrine lake plain [Qlp3]: This unit comprises 0.3 percent of the map area and represents very gently sloping areas downslope from their associated beach ridges or beach plains that were formerly submerged and affected by wave action. The Qlp3 unit is commonly covered by sand and gravel, but does not have associated identifiable beach ridges or other lacustrine constructional landforms. The age of Qlp3 unit is similar to the age of its associated beach ridge [Qbr3] at an elevation of 670 m. Therefore, the age of Qlp3 unit is poorly constrained to about 14,550 ± 850 cal yr B.P.

Lacustrine lake plain [Qlp2, Qlp2(d)]: The Qlp2 unit comprises 0.4 percent and the dissected equivalent surfaces [Qlp2(d)] encompasses 1.1 percent of the map area. The Qlp2 unit

has surface characteristics similar to those of the Qlp3 unit, but it is temporally associated with the 683 m shoreline. The largest extent of the Qlp2 unit is located in the southern sector of the map area. The Qlp2(d) unit has a high degree of surface erosion and rilling with surfaces preserved ≤2 m above surrounding topography, which exhibit a high albedo surface reflectance from either the exposure of light-colored and fine-grained lake sediments or from soluble salt efflorescence that have precipitated due to local high groundwater conditions. Most of the Qlp2(d) unit is located in the western-southwestern sector of the map area in zones that are being actively incised by active alluvial and fluvial processes. Therefore, the age of the Qlp2 unit is constrained to about 14,550 ± 850 cal yr B.P. and the geomorphic surface age of the Qlp2(d) unit is poorly constrained between 14,550 ± 850 cal yr B.P. and 2014 A.D.

Lacustrine lake plain [Qlp1, Qlp1(d), Qlp1-2]: The Qlp1, Qlp1(d), and Qlp1-2 units comprise percent, 3.1 percent, and <0.1 percent of the map area, respectively. The Qlp1 unit has surface characteristics similar to those of the Qlp2 unit, but it is temporally associated with the 690 m shoreline. The Qlp1-2 unit is a grouped unit due to poor elevation control that contains both Qlp1 and Qlp2 surfaces. The Qlp1 and Qlp1(d) units are located in the western- southwestern sector of the map area below a well-developed 690 m erosional shoreline feature cut across the Qf1 unit. The Qf4 and Qflp2 units are inset to both of these Qlp units. The Qlp1(d) unit locally exhibits evidence of channelized shallow surface flow and high reflectance from soluble salt efflorescence associated with paleospring and groundwater discharge. In the southwestern sector of the map area the Qlp1(d) unit, however, locally extends above a well-developed beach ridge at ~688 m up to an elevation of ~700 m. The units surface in this area consists of a slightly elevated (≤2 m) surface with light-colored, relatively fine-grained (sand and silt) sediment overlain by a surface lag of angular and porous calcium carbonate fragments. The fine-grained sediment likely accumulated due to trapping by standing water, wet surfaces, or phreatophytic vegetation in areas of springs, seeps, or shallow groundwater tables (Pigati *et al.*, 2014). The fragmental lag of porous calcium carbonate appears to be spring tufa as described by Pedley (1990), which provides supporting evidence of paleospring and groundwater discharge in the area or a marsh paleoenvironment associated with fluvial-deltaic deposition in areas near a lake level at 690 m. The age of the Qlp1 and Qlp1-2 units are constrained to 14,550 ± 850 cal yr B.P. and the geomorphic surface age of the Qlp1(d) unit is poorly constrained between 14,550 ± 850 cal yr B.P. and 2014 A.D.

Lacustrine beach ridge [Qbr3]: This unit comprises <0.1 percent of the map area. The Qbr3 unit is the youngest beach ridge unit found at an elevation of about 670 m and represents a former lake-surface elevation. This unit was formed by waves breaking on a shore and transporting locally available sediment into a linear pile parallel to the shoreline. The particle size distribution within and comprising the surfaces of this unit is dependent on the character of sediment available for wave transport, as well as the local wave environment (Adams and Wesnousky, 1998). The Qbr3 unit is located in the eastern sector of the map area as a poorly preserved feature across and at the base of truncated Qf2 and Qf3 units. Based on the lake-level curve of Smith (2009) the 670 m beach ridge formed immediately after the latest Pleistocene China-Searles highstand. Therefore, the age of the Qbr3 unit is about 14,550 ± 850 cal yr B.P. Beach deposits at ~670 m were sampled during this project and submitted to the Desert Research Institute's E.L. Cord Luminescence Laboratory for optically stimulated luminescence (OSL) dating. Laboratory analyses are pending at the time of issuance of this report.

Lacustrine beach ridge [Qbr1]: This unit comprises 0.1 percent of the map area and is the oldest beach ridge in China Lake basin. The Qbr1 unit is mapped near an elevation of about 690 m and represents the latest Pleistocene highstand of China-Searles Lake (Smith, 2009). Similar to the 670 m beach ridge, the Qbr1 unit does not form a continuous landform that can be traced around the entire basin, but instead occurs as isolated beach ridge remnants that have been obscured or buried by younger alluvial fans and eolian features. The best preserved Qbr1 units are located in the southwestern and southeastern sectors of the map area where they have formed at the base of shoreline scarps across the base of the Qf1 unit. The age of the Qbr1 unit is constrained to about 14,550 ± 850 cal yr B.P.

Lacustrine beach plain [Qbp3]: This unit comprises 0.4 percent of the map area. The Qbp3 unit is the youngest beach plain unit found at an elevation of about 670 m and represents a former lake-surface elevation. This unit was formed by waves breaking on a shore and transporting locally available sediment into a relatively broad zone parallel to the shoreline. Variable mixtures of sand and gravel commonly cover the Qbp3 unit. The surface morphology of this unit is typically devoid of identifiable beach ridges or other associated lacustrine constructional landforms. The largest extent of the Qbp3 unit is in the northern sector of the map area where it forms a ~2 km-long and ~0.6 km-wide, broad and gently sloping sand surface along the 670 m elevation contour. Locally, this particular feature is dissected by active channels [Qac], young and old fluvial plain [Qflp2 and Qflp1] units, and surrounded by dissected playa [Qpl(d)]. The Qbp3 unit also is present within the eastern sector of the map area where it crosses intermediate- aged alluvial fans [Qf3]. The age of the Qpb3 unit is similar to the age of the Qbr3 unit, therefore is poorly constrained to about 14,550 ± 850 cal yr B.P.

Lacustrine beach plain [Qbp2, Qbp2(d)]: The Qbp2 unit comprises 1.6 percent, whereas the dissected equivalent surfaces [Qbp2(d)] encompasses <0.1 percent of the map area. The Qbp2 unit has surface characteristics similar to those of the Qbp3 unit, but it is spatially and temporally associated with the 683 m shoreline. The largest extent of the Qbp2 unit is located in the southern and northern sectors of the map area between the elevations of 670 and 683 m. In addition, less extensive and isolated areas with preserved Qbp2 surfaces also are located in the western and eastern sectors near an elevation of 683 m. The Qbp2(d) unit is located in the southern sector of the map area adjacent to the Qbp2 unit, as well as in an area between a left- step of two active fault splays of the Little Lake fault zone. This left-step in the fault zone has produced appreciable uplift and a high degree of localized surface erosion and rilling. The undeformed Qbp2 surfaces elsewhere are relatively planar and consist of poorly developed desert pavements in the southern sector of the map area. The Qbp2 unit in the northern sector of the map area consists of a well-developed beach ridge and recessional strandline complex that extends from an elevation of about 683 m down to 677 m in the vicinity of Darwin Road. The age of the Qpb2 unit is similar to the age of the 683 m Qlp2 unit, therefore is poorly constrained to about 14,550 ± 850 cal yr B.P.

Lacustrine beach plain [Qbp1, Qbp1(d), Qbp1-3]: The Qbp1, Qbp1(d), and Qlp1-3 units comprise 1.2 percent, 2.1 percent, and <0.1 percent of the map area, respectively. The Qbp1 unit has surface characteristics similar to those of the Qbp2 unit, but it is spatially and temporally associated with the 690 m shoreline. The largest extent of the Qbp1 unit is located in the western, southern, and eastern sectors of the map area between the elevations of about 683 and 690 m,

where the unit commonly truncates the Qf1 and Qf1(gwd) units. The Qbp1(d) unit is located in the southern and southeastern sectors of the map area in an area that is bounded by the active Little Lake and Airport Lake fault zones. Similar to the Qbp2(d) unit, but over a much larger area, the surface morphology of the Qbp1(d) unit reflects appreciable uplift in the form of significant channel erosion and localized rilling across post-lake modified surfaces. Although much of the Qbp1 unit near Ridgecrest is obscured by development, dissection of the surface is evident in both developed and undeveloped areas surrounding the slopes of a subbasin playa [Qpl]. The undeformed Qbp1 surfaces elsewhere are relatively planar and consist of poorly developed desert pavements in the western sector of the map area that are closely associated with the Qbr1 unit and erosional shoreline scarps formed across the Qf1 unit. The Qbp1 unit in the northern and eastern sectors of the map area is moderately to poorly preserved due to burial by eolian features or erosion from intermediate- and young-aged alluvial fans. Locally, the upper limit of the Qbp1 unit in this sector of the basin is discernible as a prominent break-in-slope that has the form of a shoreline scarp that truncates the Qf1 unit. The age of the Qpb1unit is similar to the age of the 690 m Qbr1 unit, therefore is constrained to about 14,550 ± 850 cal yr B.P.

Lacustrine beach platform [Qbpf]: This unit comprises 0.8 percent of the map area and is characterized by relatively planar and flat to gently sloping erosional surfaces that extend from an elevation of 960 m to near 670 m. The Qbpf unit represents areas that have been affected by wave action. The Qbpf unit consists of well-developed abrasion platforms across basaltic flow [Qv] rocks in the northern sector of the map area and across the flanks of Lone Butte and other granitic [Kg] knobs and hills in the eastern sector of the map. This unit likely records the occupation and subsequent erosion from numerous lake-level oscillations that are older than the latest Pleistocene lake-level fluctuations in the basin; however, because these surfaces were last inundated and affected by the recent highstand, the Qbpf is assigned a maximum geomorphic surface age of about 14,550 ± 850 cal yr B.P.

Lacustrine beach plain (old) [Qbp(o), Qbp (o-d)]: The Qbp(o) and Qbp(o-d) units comprise percent and <0.1 percent of the map area, respectively. The Qbp(o) is identified in areas below a discernable break-in-slope at an elevation of ~700 m. The surface near the 700 m contour is interpreted to be a shoreline scarp formed by a lake level older than the 690 m shoreline. The Qbp(o) unit is identified in the northeastern sector of the map area as a poorly preserved surface that is bounded mostly by Qf2 units, as well as masked by a ubiquitous cover of eolian features. The Qbp (o-d) unit is located in the southeastern sector of the map area near the subbasin playa [Qpl] unit. Similar to other beach plain dissected units in the vicinity, the Qbp(o-d) consists mostly of closely spaced rills developed on moderately indurated, bedded, fine-grained lacustrine sediment that is older than latest Pleistocene. The map boundaries of the Qbp(o-d) unit encompass a relatively narrow and elevated ridgeline above the elevation of 690 m. The top of the ridgeline is relatively planar and at an elevation of about 700 m. Two mapped fault splays of the Airport Lake fault zone bound the ridgeline. It appears that the linear morphology of the ridgeline is tectonically controlled; because of uplift, evidence of older and higher shoreline features has been preserved. The age of the Qpb(o) unit is poorly constrained to older than 14,550 ± 850 cal yr B.P., whereas as the Qpb(o-d) is assigned a geomorphic surface age between 14,550 ± 850 cal yr B.P. and 2014 A.D.

PLAYA FEATURES [QPL, QPL(PL), QPL(C), QPL(D), QPL(I), QPL(M), QFPP, QW]

Playa features represent the accumulation of relatively fine-grained sediments (sand, silt, and clay) in the bottom of closed basins and other depressions or relatively flat areas (Peterson, 1981). Some of the larger playas [Qpl] represent the floors of former lakes where fine grained sediment accumulated while the lake was present. Playettes [Qpl(pl)] are relatively small playas that represent the accumulation of fine grained sediments from slopes immediately surrounding these features (Peterson, 1981). At China Lake, active incision of the larger playas [Qpl] by playa channels [Qpl(c)] has led to areas of dissected playa [Qpl(d)]. Many of the playas are surrounded by playa margins [Qpl(m)] that represent transition zones between distal alluvial fans and playas. Some playas have been mapped as being frequently inundated [Qpl(i)] or occupied by seasonal wetlands [Qw]. Along some of the drainages, floodplain playas [Qflp(p)] represent the ponding of sandy sediment during discharge events. Sediments associated with playas may be redistributed across the playas by fluvial incision, erosion, and transport as well as by eolian processes.

Playa [Qpl]: This unit comprises 0.3 percent of the map area. The Qpl unit represents relatively low-relief and flat to gently sloping playa surfaces of a closed basin that is periodically flooded or submerged. Playas include broad, planar expanses of the landscape covered by deposits of horizontally bedded fine sand, silt, and clay. The age of the Qpl unit is constrained to between 1850 and 2014 A.D. because Qpl surfaces are the site of historical deposition and inundation.

Playa channel [Qpl(c)]: This unit comprises 0.2 percent of the map area. The Qpl(c) unit includes stream channels incised into the playa. The playa channels commonly, but not always, originate on the surrounding piedmonts. Some playa channels head on the playa itself. A thin layer of sand may accumulate in playa channels, but many channels appear to be cut directly into the Qpl surface and contain no fluvial sediment. Playa channels typically are straight to sinuous and their networks have an overall dendritic pattern. The age of the Qpl(c) unit is constrained to between 1850 and 2014 A.D., because Qpl(c) channels are the site of historical deposition.

Dissected Playa [Qpl(d)]: This unit encompasses 6.5 percent of the map area and includes playa areas that have been dissected by the Qpl(c) unit. The Qpl(d) unit surfaces are no longer subject to active playa deposition. The timing of playa incision is unknown but may be recent. Therefore, the age of the Qpl(d) unit is poorly constrained to between ~4,200 cal yr B.P. and 2014 A.D.

Playette [Qpl(pl)]: This unit comprises 1.6 percent of the map area. The Qpl(pl) unit represents small playas that are found in small closed depressions on the margins of larger playas or within delta plain and alluvial fan units. The surfaces of the Qpl(pl) unit are flat and generally composed of sand, silt, and clay that represent the recent transport and deposition of sediment from slopes immediately surrounding the playette during precipitation events. Therefore, the age of the Qpl(pl) surfaces are constrained to between 1850 and 2014 A.D.

Playa subjected to frequent inundation [Qpl(i)]: This unit includes 1.0 percent of the map area and includes those parts of the playa that are frequently inundated on an annual basis or remain inundated for longer periods. Many of the Qpl(c) units terminate within the Qpl(i) unit. The deposits associated with this unit are comprised dominantly of silt and clay. The age of the Qpl(i) unit is constrained to between 1850 and 2014 A.D.

Playa margin [Qpl(m)]: This unit comprises 0.8 percent of the map area. The Qpl(m) unit includes areas that are adjacent to the playa and form the transition between the playa and distal alluvial fan environments, therefore surfaces are expected to be silt- and sand-rich with abundant soluble salts. The Qpl(m) unit commonly contains areas of sand sheet feature types [Qe(ss) and Qe(ssv)]. Based on the spatial relationships between the Qpl and youngest Qf5 units, the age of the Qpl(m) unit is constrained to ~4,200 cal yr B.P. and 2014 A.D.

Seasonally inundated wetlands [Qw]: This unit includes 1.8 percent of the map area. The Qw unit represents parts of the playa that are seasonally inundated by storm runoff and maintained by natural spring discharge and/or anthropogenic discharge. The age of Qw surfaces are composed mostly of standing water and may contain paleospring deposits, therefore this unit is constrained between 1850 and 2014 A.D.

BEDROCK UNITS

Bedrock is exposed in the northwestern part of the mapping area and the southeastern part of China Lake near the sill. Bedrock in both areas has played a role in the hydrologic history of China Lake. Bedrock in the northwestern map area consists of well-preserved Quaternary basalt flows that contain erosional shoreline features in the form of beach platforms and wave-cut notches that extend from 690 m to above 675 m. On the eastern margin of China Lake, Cretaceous granitic rock (Kg) presumably forms the sill that has controlled outflow of China Lake into the Searles Lake basin, which also records past lake levels in the form of beach platforms and wave-cut notches that also extend from an elevation about 690 down to near 670 m.

Basaltic Rocks [Qv]: The Qv bedrock unit includes 0.1 percent of the map area and consists of volcanic rocks in the form of basaltic lava flows at the distal flanks of the Coso Range in the northwestern part of the mapping area.

Granitic Rocks [Kg]: The Kg bedrock unit comprises 1.2 percent of the map area and consists of intrusive granitic rocks of Mesozoic age that commonly forms small buttes and hills in the southeastern part of the mapping area.

ANTHROPOGENIC FEATURES [AN(R), AN]

Below the 700 m contour there are large areas of human modification and disturbance of the landscape in the form of roads and their embankments, buildings, other infrastructure, and bladed areas. In some places, but not all, it was possible to infer the geology and geomorphology of disturbed areas.

Roads [An(r)]: This unit includes paved and unpaved roads.

Other anthropogenically disturbed areas [An]: This unit includes surfaces that have been disturbed or have been developed.

This page intentionally left blank.

Appendix B

THE BROADER HYDROLOGIC AND GEOMORPHIC CONTEXT OF CHINA LAKE

(This appendix was composed by Kenneth D. Adams, Steven N. Bacon,
David L. Decker, and Thomas F. Bullard)

This page intentionally left blank.

INTRODUCTION

It is important to gain an understanding of the broader hydrologic and geomorphic context within which the China Lake basin is located in order to develop a complete late Pleistocene and Holocene history of the lake. China Lake was at times one of several lakes connected by the paleo-Owens River, extending from the Owens Lake outlet to the Panamint Valley during the last glacial/pluvial cycle (<30 ka) (Figure 1 and Plate B-1) (Smith and Street- Perrott, 1983). The timing and nature of these connections provides the context within which to interpret the hydrologic and cultural history of China Lake.

New preliminary evidence synthesized with data and results from existing studies (*e.g.*, Duffield and Smith, 1978; Saint-Amand, 1987; Cerling, 1990; Bacon *et al.*, 2006; Phillips, 2008; Smith, 2009; Meyer *et al.*, 2011; Amos *et al.*, 2013) indicates that there were at least one and possibly several, large floods caused by repeated failures of the Owens Lake sill (Bacon *et al.*, 2014). Although the nature of the failures and resulting style of discharge (single large burst or long-term sustained, above "average" discharge) is not yet known, it is apparent that these floods resulted in large volumes of water flowing down the paleo-Owens River channel into the China-Searles Lake basin. Evidence for significant flooding comes from abrupt changes in the Owens Lake-level curve (Bacon *et al.*, 2006), scour features and flood debris fans along the paleo- Owens River channel (Amos et al, 2013; Bacon *et al.*, 2014), and lacustrine features in China Lake, Salt Wells Valley, and Searles Lake (Smith, 1968, 2009; Smith and Street-Perrott, 1983) (Plate B-1).

Although it is enticing to invoke single or multiple catastrophic floods resulting from failure of the Owens Lake sill, it must be pointed out that there are multiple scenarios, including a range of stream discharges and sediment transport modes that could explain the presence of the debris fans. Each scenario has implications for understanding the hydrology in the China Lake basin, such as the distribution of fluvial, lacustrine, and eolian deposits in the subsurface and their relation to groundwater hydrology. Some example scenarios include (1) long-term, low- flow conditions that persisted during periods of connection of Owens and China lakes; (2) prolonged periods of sustained high-flow that resulted in channel widening, high shear stresses on the channel bottom and margins, and bedload that allowed the river to cut into resistant bedrock units, (3) periodic large floods that could have occurred during periods of low flow conditions and/or during periods of high flow conditions, (4) periodic mobilization of large volumes of very coarse sediment coincident with flooding, and (5) possible large floods associated with failure of the sill between Owens Lake and China Lake (e.g., Bacon *et al.*, 2014).

The following discussion is limited to the fluvial system between Owens Lake and China Lake where we review the preliminary evidence only in the context of large, catastrophic flooding and present testable hypotheses about the timing, number, and magnitudes of floods. A companion study (Bacon *et al.*, 2014) is focusing on revising the lake-level and overflow history of Owens Lake and those results will be integrated with results of the present study to develop a more comprehensive view of this integrated hydrologic system. Other hydrologic scenarios that could lead to observed erosional and depositional features are not presented at this time.

GEOMORPHOLOGY OF THE PALEO-OWENS RIVER CHANNEL

The geomorphology of the paleo-Owens River channel records abundant evidence of large magnitude flow along its 65 km length from the Owens Lake sill area near the Haiwee reservoirs downstream through Rose Valley and Fossil Falls and into China Lake (Plate B-1). The following sections presents this evidence for the fourth possibility, large catastrophic floods, beginning at the upstream end of the paleo-channel and ending at China Lake.

ROSE VALLEY AND FOSSIL FALLS REACH

To help explain large-scale erosional and depositional features identified in the outlet area of Owens Lake and within the China-Searles Lake basin, Phase II fieldwork included a reevaluation of the magnitude of potential discharge in the area of Fossil Falls.

Fossil Falls and a large cinder cone (Red Hill) are prominent physiographic features within Rose Valley that disrupt stream flow along the paleo-Owens River. Amos *et al.* (2013) recently revised the mapping and age determinations for two basalt flows near Red Hill of Duffield and Smith (1978) to be ~62 ka (Qb3) and ~200 ka (Qb2) (see Appendix BB-1), as well as identified and dated large-scale flood features at, and downstream of Fossil Falls (Figure B2).

Fossil Falls, which consists of a narrow, deep cut through basalt flows, has long been recognized as evidence for a large river flowing along this path (*e.g.*, Duffield and Smith, 1978; Saint-Amand, 1987; Cerling, 1990; Amos *et al.*, 2013). The fluvial morphology present within the 20-m wide cascading reach of the active channel at Fossil Falls includes water-sculpted columns and deep “potholes” eroded into basalt, before the channel abruptly descends about 25 m through a deep notch (Saint-Amand, 1987) (Figure B1).

The mapping of Amos *et al.* (2013) indicates that stream flow may have bifurcated around Red Hill and been as wide as 1.5 km immediately downstream of Fossil Falls (Figure B2). Our reconnaissance-level field observations and examination of aerial imagery (Google Earth and ArcGIS) show that there are a number of depositional and erosional features that confirm this interpretation. For example, northwest of Red Hill and southeast of Fossil Falls features interpreted to be fluvial trimlines constrain the maximum width of the flow (Figure B2). Upstream and east of Fossil Falls, the Qb2 and Qb3 basalt surfaces are scoured into a series of elevated and interconnected channels in a zone ~1 km-wide that displays scabland morphology (*i.e.*, irregularly scoured bedrock surfaces stripped of surficial deposits), albeit at a much smaller scale than features associated with the channeled scablands of east-central Washington State (*e.g.*, Baker, 2009).

FIGURE B-1. View Upstream of Active Channel at Fossil Falls. Note the potholes and eroded Qb3 basalt, both indicative of focused, high-energy discharge.

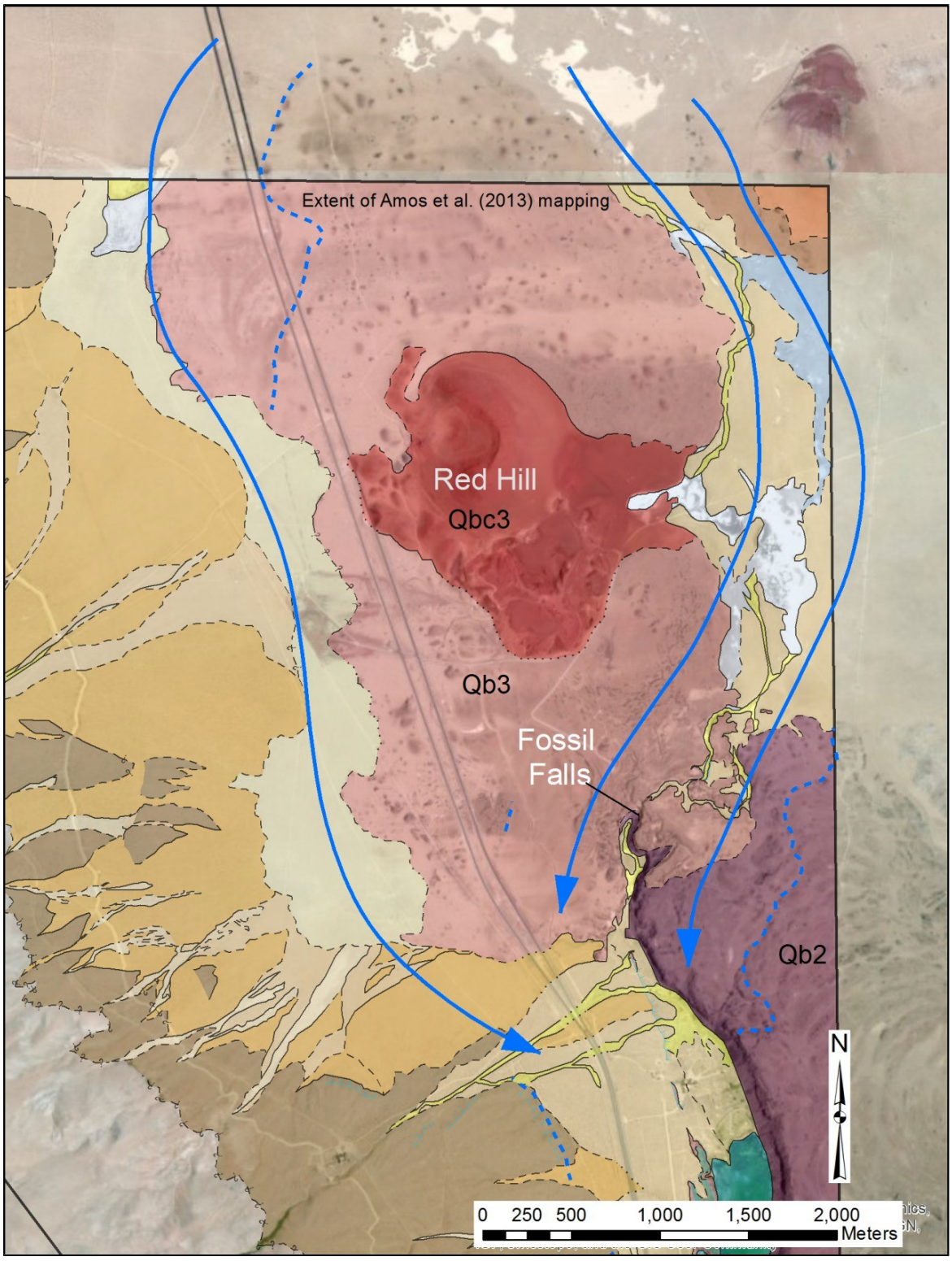

FIGURE B-2. Geologic Map (After Amos *et al.*, 2013) of Fossil Falls Area Showing Distribution of Qb2 and Qb3 Basalts, Flood Trimlines (Dashed Blue Line), and presumed Flow Lines of Floods (Solid Blue Lines).

Southeast of Fossil Falls, the edge of the escarpment formed in the Qb2 basalt above the paleo-Owens River channel is eroded by a number of short channels terminating in steep-sided amphitheaters that have negligible contributing drainage basins. The steep bedrock channels suggest high-energy discharge as a likely process for their formation, as suggested by previous workers (Duffield and Smith, 1978; Saint-Amand, 1987; Amos *et al.*, 2013). Supporting evidence for large discharge outside of the active channel at Fossil Falls comes from the distribution of a patchy gravel deposit covering the Qb2 and Qb3 surfaces on either side of the active channel that consists of abundant small (< 3cm), rounded, granitic clasts. It is noted that Duffield and Bacon (1981) report that granitic xenoliths are common within the basalt of Red Hill (Qb3) and that rounded gravel was ejected during eruptions of Red Hill. As observed during Phase II field visits, however, the gravel deposit lacks large amounts of scoria erupted from Red Hill, thereby indicating that it is likely not a cinder cone ejecta deposit. No granitic clasts were observed within the Qb3 basalt; instead the granitic clasts were deposited on top of the basalt. Furthermore, the rounded granitic clasts (1-3 cm) and position of the gravel deposit adjacent to but above well-developed channels indicates that they were probably deposited by flowing water associated with the paleo-Owens River.

CONFINED AND UNCONFINED REACHES BELOW FOSSIL FALLS

In addition to investigating the inferred flood morphology at Fossil Falls, the course of paleo-Owens River channel was also examined downstream to the 690 m contour in Indian Wells Valley to characterize the magnitude of potential floods within confined and unconfined reaches. The course of the former river channel is oriented mostly north-south and is bordered on the east by an extensive terrace capped by basalt (Qb1 unit; ~250 to 400 ka) that is underlain by older, distal alluvial fan deposits shed from the Sierra Nevada and on the west by granitic bedrock and the piedmont of the Sierra Nevada (Duffield and Bacon, 1981; Amos *et al.*, 2013).

Confined Reach of Paleo-Owens River Channel Below Fossil Falls

Younger basaltic units (Qb2 and Qb3) erupted in the vicinity of Red Hill, followed the course of the paleo-Owens River channel toward China Lake for a distance of about 16-18 km, each leaving a relatively thick (5-10 m), intercanyon basalt flow with well-developed columnar joints (Duffield and Bacon, 1981; Amos *et al.*, 2013). The older Qb2 unit is exposed at the distal end of the confined paleo-Owens River channel where it has been scoured and eroded into a large amphitheater-shaped dry falls, first noted by Duffield and Smith (1978) (Figure B3). The upstream propagation of this headcut resulted in a ~150-m wide and ~1-km long channel excavated through the Qb2 unit, which locally is composed of basalt at least 8 m thick.

The younger basalt (Qb3) was erupted from the base of Red Hill (Figure B2), and followed the paleo-Owens River channel downstream for ~16 km (Duffield and Smith, 1978; Duffield and Bacon, 1981; Amos *et al.*, 2013). Most of this lava flow has been eroded, leaving scattered remnants along the length of the channel. The Qb3 unit is about 4-10 m thick (Duffield and Bacon, 1981).

In addition to the intercanyon basalts, Amos *et al.* (2013) also dated deposits associated with two terraces below Little Lake Narrows to be in the range of 64 ± 5.6 ka based on ^{10}Be cosmogenic surface exposure dating. Remnants of these two terraces extend greater than 5 km downstream and their deposits consist of basaltic and granitic boulders up to several meters in diameter on a strath terrace cut on Qb3. Surface morphology of the terraces consist of poorly preserved and moderately developed linear to curvilinear boulder- and block-rich surfaces separated by intervening channels.

FIGURE B-3. Amphitheater-Shaped Dry Falls Formed on Columnar Qb2 Basalt Within Paleo-Owens River Confined Channel. The minimum height of the dry falls is about 7-8 m.

The magnitude of discharge in the paleo-Owens River channel required to form propagating headcuts, amphitheater-shaped falls, and extensive bouldery terraces is consistent with large-scale flooding (*e.g.*, O'Connor, 1993; Amos *et al.*, 2013; Lamb *et al.*, 2014). Alternatively, some of the same features could be produced by sustained, high discharge during periods of prolonged spilling from Owens Lake during deglaciation of the Sierra Nevada or other wet periods of climate during the latest Pleistocene.

Unconfined Reach of PALEO-Owens River Channel to the 690 M Contour in the China Lake Basin

At the distal end of the paleo-Owens River channel, where it becomes unconfined upon entering Indian Wells Valley, three distinct large-scale flood debris fan features (Qfdf3, Qfdf2, Qfdf1; Appendix BB-1) were identified during Phase II field investigations. All three flood debris fans are younger than about 62 ka, the age of Qb3 (Amos *et al.*, 2013), and are assigned relative ages with respect to each other based on their cross-cutting relations. The flood debris fans are composed of thick accumulations of basaltic and granitic boulders and blocks and their surface expression has the form of a well-expressed network of distributary linear to curvilinear boulder-rich levees separated by deep intervening channels. These levees are similar in form and size to debris levees described on the Sierra Nevada piedmont near Lone Pine that are attributed to outburst flooding (e.g., Benn *et al.*, 2006). The largest basaltic block (7 m x 6 m x 5 m) was observed resting on a strath terrace (Qt1) cut into the oldest flood debris fan (Qfdf1) and the Qb2 basalt unit (Figure B4). The largest granitic boulders observed on the Qt1 surface were 1-2 m in diameter (Figure B5).

The three large-scale flood debris fan features have been mapped as Quaternary alluvial fans (Qf) and specifically into debris flood fans (Qfdf). The relief on the oldest debris flood fan unit (Qfdf1) is about 20 m, measured from the fan's apex to its distal edge. The abundant granitic boulders intermixed with the basaltic boulders and blocks, as well the presence of linear to curvilinear boulder- and block-rich levees indicate that Qfdf1 is a large-scale alluvial deposit that overlies the Qb2 basalt and not the Qb2 basalt itself (Figure B6), as previously mapped by Duffield and Smith (1978), Duffield and Bacon (1981), and Amos *et al.* (2013).

The intermediate-age flood debris fan unit (Qfdf2) is inset within the Qfdf1 unit and is found within the channel on either side of the farthest downstream outcrops of Qb3, as well as in fan-shaped deposits downstream of the amphitheater-shaped dry falls (Figure B6). The surfaces of the Qfdf2 unit also express a well-developed network of distributary boulder levees and intervening channels. Basaltic boulders and blocks on the Qfdf2 are slightly smaller than those on Qfdf1, but still attain sizes of several meters. The Qfdf2 unit also contains abundant granitic boulders and extends downstream to an elevation of about 720 m at its distal end.

FIGURE B-4. Large (7 m x 6 m x 5 m) Basalt Boulder on Qt1 Surface. Primary flow texture in the boulder indicates an orientation inconsistent with a bedrock outcrop. Person for scale.

FIGURE B-5. Large Basalt Boulders and Smaller (0.5 to 1 m) Granitic Boulders Resting on Scoured Qb2 Basalt Upstream From Amphitheater-Shaped Dry Falls Shown in Figure B3. Rock pick (0.5 m) for scale.

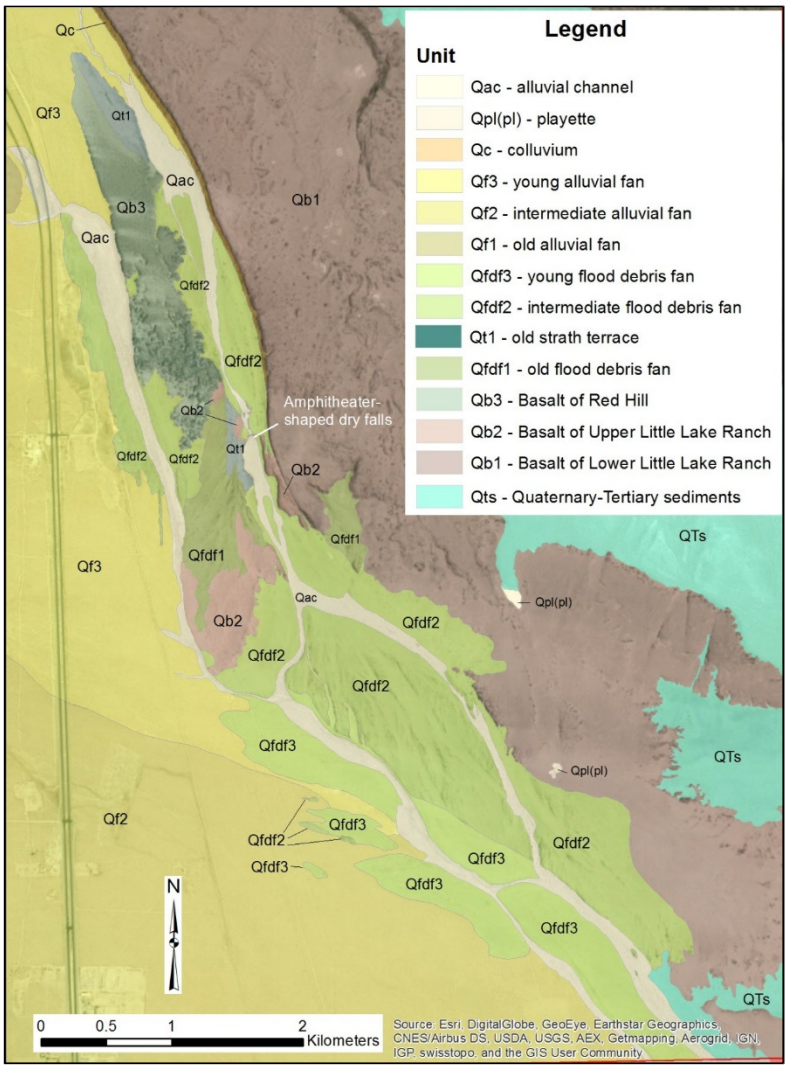

FIGURE B-6. Preliminary Geomorphic Map Upriver of Inlet Area of China Lake Shows Distribution of Units in Relation to Paleo-Owens River Channel (Mapping K. Adams).

The southwestern edge of the $Qfdf_2$ unit is truncated by the $Qfdf_3$ unit, which demonstrates that $Qfdf_3$ is the youngest of the flood debris fans (Figure B6). Although the $Qfdf_3$ unit is finer-grained than the two older debris flood fan units, the unit does contain basaltic and granitic boulders several meters in diameter. The surface of $Qfdf_3$ is largely covered by younger sandy and gravelly alluvium, but natural exposures in channel walls cutting the unit show $Qfdf_3$ to be underlain by sandy gravelly boulder to bouldery gravel deposits. Phase II field observations indicate that the boulders in the $Qfdf_3$ unit become finer grained and less frequent downstream, but can still be traced to, but not below, the latest Pleistocene highstand elevation of 690 m in China Lake basin and a fault splay of the Little Lake fault zone.

The broad extent, fan-shaped surface morphology, and high concentration of large boulders and blocks on the surface of all three Qfdf units are indicative of debris flood deposits. The large-scale morphology of the flood debris fans implies very large discharges and high sediment load from the confined reaches of the paleo-Owens River.

PRELIMINARY CONCLUSIONS AND TESTABLE HYPOTHESES OF LARGE-SCALE FLOODING

The geomorphic and hydrologic history of China Lake is complex and cannot be sufficiently understood without viewing it in a broader regional context. Reconnaissance-level investigation along the path of the paleo-Owens River from Owens Lake reveals fluvial evidence for erosion of bedrock and the transport and deposition of large boulders.

Evidence for large-scale flooding includes scoured and eroded basalt flows, interpreted fluvial trim lines well above the base of the paleo-Owens River channel, fluvial gravel above and outside well developed channels at Fossil Falls, and flood debris fans (Figure B6 and Plate 1).

Further work is needed to identify and confirm the presence of paleo-Owens River flood deposits in China Lake basin. These observations form the basis for testable hypotheses concerning the paleohydrology of the China Lake basin that include:

a.) Multiple floods flowed down the paleo-Owens River channel into the China Lake basin during the late Pleistocene and possibly early Holocene. *Test: Date the different flood debris fans and fan delta units with cosmogenic surface exposure dating, luminescence, or other appropriate dating method.*

b.) The features and deposits created by these flow events were the result of large magnitude floods and not sustained, "above average" flows. *Test: Use hydraulic and sediment transport models (e.g., O'Conner and Webb, 1988; Baker, 2009; Lamb et al., 2014) to estimate the magnitude of discharge during these events.*

Determining the timing and nature of floods impacting the China Lake basin may have important implications for the distribution and age of archaeological sites at NAWS China Lake because it is possible that one or more of these floods occurred after the first people entered the basin.

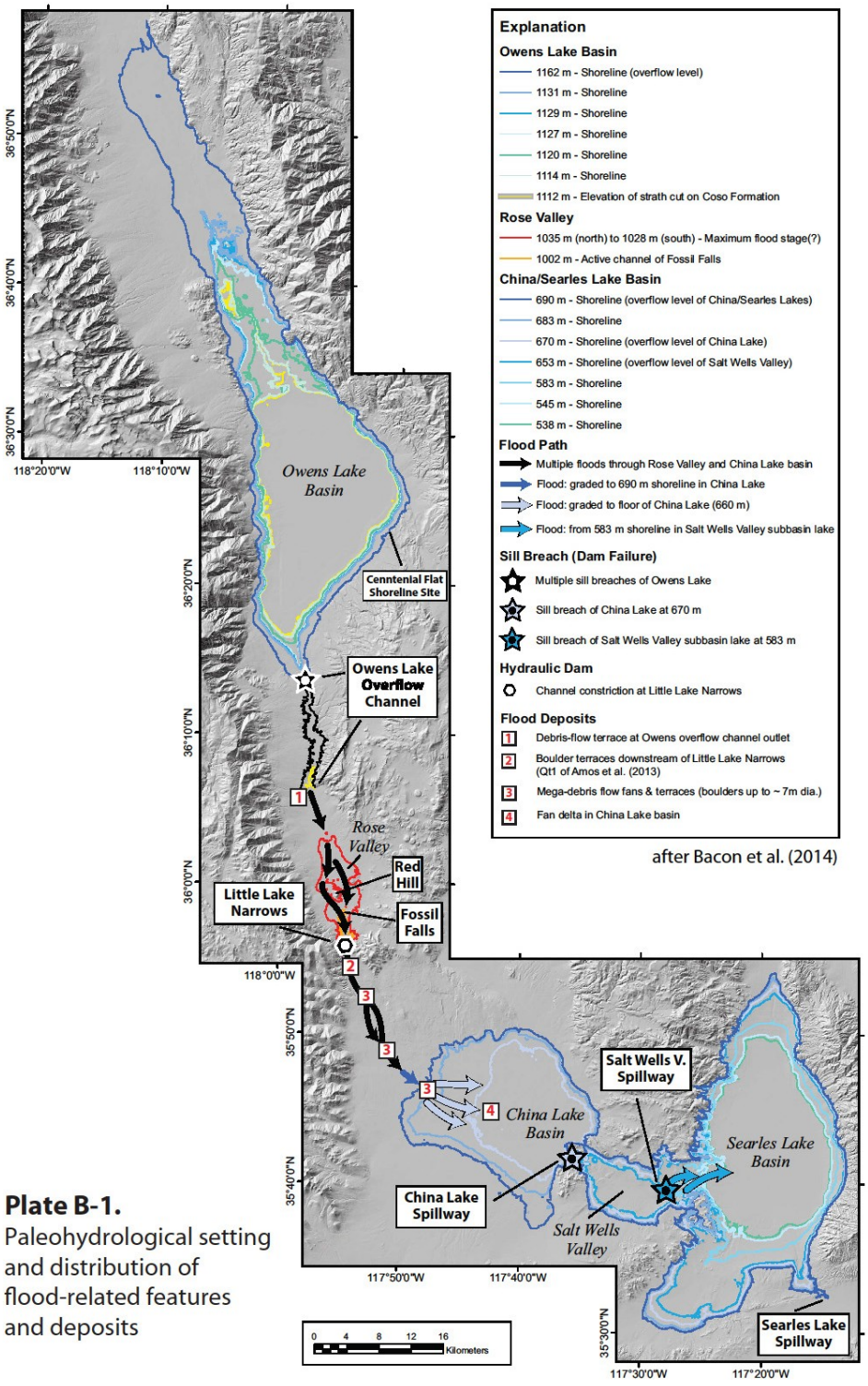

Plate B-1.
Paleohydrological setting and distribution of flood-related features and deposits

PLATE B-1. Paleohydrological Setting and Distribution of Flood Sediments and Features Along Paleo-Owens River and in China-Searles Basin.

This page intentionally left blank.

Appendix C

UNIT DESCRIPTIONS

This page intentionally left blank.

UNIT DESCRIPTIONS

Flood debris fan [Qfdf3]: In the context of a catastrophic flood scenario, flood debris fan [Qfdf3] is the youngest flood debris fan unit in the study area and is observed only in the northwestern part of the mapping area above an elevation of 690 m. Qfdf3 occupies broad interfluves dissected (<5 m) by channels of the paleo-Owens River whose surfaces are largely covered by sand and fine gravel. In places, however, prominent distributary boulder bars composed of Qb2 and Qb3 basalt boulders (< 2.5 m) and smaller granitic boulders ($\leq$ 1 m) are present on the surface (Figure B4). Few Natural exposures in channel walls show the surface to be underlain by sandy gravelly boulder to bouldery gravel deposits. Phase II field observations indicate that the boulders in the Qfdf3 unit become finer grained and less frequent downstream, but can still be traced to, but not below and across a prominent fault splay of the Little Lake fault zone at an elevation of the 690 m highstand shoreline in China Lake basin. Until additional geomorphic data and direct numerical ages are collected, the age of the Qfdf3 unit can be constrained to younger than the Qb3 basalt and older than or the same age as the 690 m highstand shoreline. Therefore, Qfdf3 is poorly constrained between younger than ~62 ka and older than or equal to 13,700 to 15,400 cal yr B.P.

Flood debris fan [Qfdf2]: The intermediate flood debris fan is inset to unit Qfdf1 and is found covering parts of the channel floor upstream and downstream of the amphitheater-shaped dry falls near where the paleo-Owens River channel becomes unconfined (Figure B6); it is also found downstream in large fan-shaped lobes separated by young alluvial channels [Qac]. The Qfdf2 unit may be correlative with one of the terrace units mapped upstream within the paleo-Owens River by Amos *et al.* (2013) and extends downstream to an elevation of about 720 m. The surface of Qfdf2 is composed of a well-developed network of distributary boulder levees composed of Qb2 and Qb3 basalt and intervening channels. Basaltic boulders and blocks on Qfdf2 are slightly smaller than those on Qfdf1, but still attain sizes of several meters in diameter. The Qfdf2 unit also contains abundant granitic boulders up to 2 m in diameter (Figure BB1).

Until additional geomorphic data and direct numerical ages are collected, the age of the Qfdf2 unit can be constrained to younger than the Qb3 basalt and Qfdf1 unit and older than the Qfdf3 unit. As a result, Qfdf2 is poorly constrained between younger than ~62 ka and older than 13,700 to 15,400 cal yr B.P. Given the observation of Amos *et al.* (2013) that there are two distinct and similar-aged debris terrace units upstream, however, the Qfdf2 unit may have a correlated age closer to ~62 ka and represent the downstream and unconfined extent of the same flood deposit.

FIGURE C-1. Large Basalt Boulders, With Fewer Granitic Boulders, Deposited as Inset Bars and Adjacent Levees With Finer-Grained Sediment Within Intervening Distributary Channels and Sideslopes on Qfdf2 Unit. Basalt boulders in foreground are 1.5 to 2 m in diameter.

Flood debris fan [Qfdf1]: The oldest flood debris fan is located at the distal end of the paleo-Owens River channel where it first becomes unconfined. This fan is characterized by bouldery distributary bars that contain large (≤ 7 m diameter) basalt boulders (Figure B4) and granitic gravel and boulders up to several meters in diameter (Figure B5). The relief on $Qfdf_1$ is about 20 m, measured from the fan's apex to its distal edge. The abundant granitic boulders intermixed with the basaltic boulders and blocks, as well as the presence of linear to curvilinear boulder- and block-rich levees indicate that $Qfdf_1$ is a large-scale alluvial deposit that overlies the Qb2 basalt; this is in contrast to previous mapping by Duffield and Smith (1978), Duffield and Bacon (1981), and Amos *et al.* (2013) that identified it as Qb2. The orientation of lava flow fabric indicators (e.g., elongated vesicles and foliation) in basaltic rocks is used to distinguish between *in situ* lava flows from large boulders and blocks transported by fluvial and colluvial processes. Fabric associated with in situ lava flows typically is oriented parallel to the ground surface; whereas, flow fabric associated with transported boulders and blocks has random orientations. The observed random orientation of flow fabric in the basalt boulders in Qfdf1 (Figure B4) supports the notion of boulder reorientation during transport in contrast to primary lava flow emplacement. Similar to the other flood debris fan units, until additional geomorphic data and direct numerical ages are collected, the age of the Qfdf1 unit can only be constrained to younger than the Qb3 basalt and older than the Qfdf2 unit. As a result, Qfdf1 is poorly constrained between younger than ~62 ka and older than 13,700 - 15,400 cal yr B.P. Given the observation of Amos *et al.* (2013) that there are two

distinct and similar-aged debris terrace units, however, the Qfdf1 unit may have a correlated age closer to ~62 ka and represent the downstream and unconfined extent of the same flood deposit.

Old fluvial terrace [Qt1]: The old fluvial terrace unit (Qt1) is mapped along the paleo-Owens River channel near where it becomes unconfined in northwestern Indian Wells Valley (Figure B6). The Qt1 terrace unit represents fluvial erosion into Qb2 and Qb3 basalts (*e.g.*, Burbank and Anderson, 2012). The Qt1 terrace is characterized by flood-scoured basalt bedrock surfaces with occasional large basalt boulders (≤ 7 m) (Figure B4, B5) and smaller granitic boulders (<2 m) scattered across its surface. The large (~7-6 m diameter) boulders may represent a boulder lag associated with erosion into the older Qfdf1 unit. The age of Qt1 is poorly constrained to younger than ~62 ka and older than 13,700 - 15,400 cal yr B.P.

BEDROCK UNITS

Bedrock is exposed in the northwestern part of the mapping area and the southeastern part of China Lake near the sill. Bedrock in both areas has played a role in the hydrologic history of China Lake. Bedrock in the Fossil Falls area and downstream consists of a series of Quaternary basalt flows that comprise Fossil Falls (Qb2, Qb3) and have flowed down the paleo- Owens River toward the China Lake basin (Qb1, Qb2, and Qb3).

Basalt Flows [Qb1, Qb2, Qb3]: Basalt flow units are described together because all three units are middle to late Quaternary in age (~300 – 60 ka) and consist of basalt flows erupted from the western flank of the Coso Range (Duffield and Smith, 1978; Duffield and Bacon, 1981; Amos *et al.*, 2013). Qb1 is referred to as the Basalt of Lower Little Lake Ranch (Duffield and Smith, 1978; Amos *et al.*, 2013) and is moderately porphyritic, containing 10 – 20 percent phenocrysts (< 3 mm) of plagioclase, with lesser amounts of olivine, and clinopyroxene. Qb1 is comprised of two discrete flows (3 - 5 m thick) that erupted from a cinder cone along the Little Lake fault zone (Duffield and Smith, 1978; Amos *et al.*, 2013) and flowed to the SSE along the floor of the paleo-Owens River channel. Recent $^{40}Ar/A^{39}Ar$ ages for the upper and lower flow units are 212 $\pm$ 14 ka and 281 $\pm$ 4 ka, respectively (Amos *et al.*, 2013). Because of subsequent erosion along the paleo-Owens River channel, Qb1 now caps a terrace along the east side of the channel that ranges in height from about 150 m near the Little Lake narrows to less than 20 m high near the lower dry falls (Figure B6) and overlies alluvium shed from the Sierra Nevada (Duffield and Smith, 1978; Amos *et al.*, 2013). Qb2 is referred to as the Basalt of Upper Little Lake Ranch and is characterized by just 1 – 2 percent of plagioclase and olivine phenocrysts (1-2 mm) (Duffield and Smith, 1978). Qb2 was erupted from a cinder cone about 5 km east of the paleo-Owens River channel and first flowed west to the channel, where it is about 70 m thick, and then continued to flow about 15 km south toward China Lake, where it crops out in the bottom of the channel, forming the rim of the lower horseshoe-shaped amphitheater (Figures B3 and B6).

Amos *et al.* (2013) used $^{40}Ar/A^{39}Ar$ techniques to generate an age of 197 ± 11 ka for Qb2. The youngest basalt flow in the area is the Basalt of Red Hill (62 ± 3 ka; Amos *et al.*, 2013), which was erupted from the Red Hill cinder cone immediately north of Fossil Falls. Petrographically, Qb3 is similar to Qb1 in that it also contains 10 – 20 percent plagioclase, olivine, and clinopyroxene phenocrysts (< 3 mm). Qb3 is distinguished from Qb1, however, by its geomorphic position in the bottom of the paleo-Owens River; whereas, Qb1 caps a high terrace to the east of the channel (Duffield and Smith, 1978; Amos *et al.*, 2013).

INITIAL DISTRIBUTION

1 Defense Technical Information Center, Fort Belvoir, VA
2 Desert Research Institute, Reno, NV (Decker, D.)

ON-SITE DISTRIBUTION

2 Code 4F0000D (archive copies)
1 Code 4G0000D (file copy)
2 Code 52000MD, Boggs, M.
2 Code 52F00MD, Penix, S.